minerals

MDPI

Article

Silver(I) Recovery by Ion Flotation Process from Aqueous Solutions in Cells with Spargers

Laura P. Ángeles Palazuelos [1], Mizraim U. Flores Guerrero [2], Miguel Pérez Labra [1], Iván A. Reyes Domínguez [3], Ramiro Escudero García [4], Francisco Patiño Cardona [5], Francisco R. Barrientos Hernández [1], Julio C. Juárez Tapia [1] and Martín Reyes Pérez [1,*]

1 Area Academica de Ciencias de la Tierra y Materiales, Universidad Autónoma del Estado de Hidalgo, Mineral de la Reforma 42186, Mexico; laura_angeles_palazuelos@yahoo.com (L.P.Á.P.); miguel_perez5851@uaeh.edu.mx (M.P.L.); profe_3193@uaeh.edu.mx (F.R.B.H.); jcjuarez@uaeh.edu.mx (J.C.J.T.)
2 Area de Electromecanica Industrial, Universidad Tecnológica de Tulancingo, Tulancingo 43642, Mexico; mflores@utectulancingo.edu.mx
3 Instituto de Metalurgia, Universidad Autónoma de San Luis Potosí, San Luis Potosí 78210, Mexico; alejandro.reyes@uaslp.mx
4 Instituto de Investigaciones Metalúrgicas, Universidad Michoacana de San Nicolás de Hidalgo, Morelia 58030, Mexico; ramiro1963@gmail.com
5 Ingenieria en Energia, Universidad Politécnica Metropolitana de Hidalgo, Tolcayuca 43860, Mexico; franciscopatinocardona@gmail.com
* Correspondence: mreyes@uaeh.edu.mx

Abstract: Extractive metallurgy has recently turned its attention to waste treatment for the recovery of precious metals through innovative metallurgical processes, such as ion flotation. This work studied the influence of several chemical and physical factors, such as the concentration of xanthate [x], frother agent [e], dithiophosphate [xl], pH, superficial gas velocity Jg, percentage of gas holdup Eg, bubble diameter (Db) calculated with the drift flux model, and the type of sparger, in the efficiency of silver(I) recovery by the ion flotation technique in sub-aerated cells. The results obtained indicate a 90.7% v/v recovery of silver(I) under conditions of 3.77×10^{-4} M [x], 1.25×10^{-4} M [e], Jg 0.5 cm/s, Jl 0.19 cm/s, Eg of 4.1% v/v, and Optimal Db of 0.11 cm, with a rigid bubble generator, achieving an apparent flotation kinetics of 4.16 1/min. The use of combinations [x]–[xl] achieve a silver(I) recovery of 86.9% with a Jg of 1.0 cm/s. The best recovery efficiencies achieved 93% w/w silver(I) are with pH 8.0, [e] of 1.25×10^{-4}, Jl of 0.19 (cm/s) and a rigid sparger compared to a flexible one.

Keywords: silver; ion flotation; gas holdup; xanthate; drift flux model

Citation: Palazuelos, L.P.Á.; Guerrero, M.U.F.; Labra, M.P.; Domínguez, I.A.R.; García, R.E.; Cardona, F.P.; Hernández, F.R.B.; Tapia, J.C.J.; Pérez, M.R. Silver(I) Recovery by Ion Flotation Process from Aqueous Solutions in Cells with Spargers. *Minerals* **2023**, *13*, 572. https://doi.org/10.3390/min13040572

Academic Editors: Weiping Liu, Savaş Özün, Xinbo Yang and Qingming Feng

Received: 4 March 2023
Revised: 5 April 2023
Accepted: 13 April 2023
Published: 19 April 2023

1. Introduction

Ion flotation technique is applied in the mining–metallurgical industry to concentrate, recover, or remove metallic ions, such as those of the platinum group [1], silver(I) [2–5], copper(II) [6], uranium(II) [7], nickel(II) [8], to separate rare earth elements [9], or the elimination of various metallic elements present in diluted aqueous solutions [10]. In addition to its versatility, this technique is economical and practical, and it can be used to eliminate toxic elements from residual effluents with a focus on green ion flotation [11].

Recent advances in ionic flotation focus on studying the type of devices, bubble generators and collectors' flotation, to improve selectivity, efficiency, low cost, and find reagents that are friendly to the environment, as studied in this present research article [2,12,13].

The separation of diluted aqueous solutions precious metal by ion flotation (IF) techniques has positioned itself in extractive metallurgy as an efficient and widely used method for the recovery or elimination of species from diluted aqueous solutions [14–17]. In the process, it uses xanthate as a collector [2,6,18] and the addition of surfactants to aqueous systems to carry out the recovery of heavy metal ions [19].

Ion flotation is defined as a technique that is based on the special properties that characterize the interfaces for the concentration of ions or other electrically charged entities contained in the aqueous phase by modifying the chemical and physical properties of the solution by effect from the addition of collectors, promoters, and frother, forming a water-soluble hydrophobic metal-collector product [14].

On the other hand, surfactants are compounds that possess a lipophobic head and a lipophilic "tail" chain group consisting mainly of an alkyl with 10 or 20 carbon atoms, which have a strong affinity for both hydrophobic and hydrophilic species [20]. The greater the length of the hydrocarbon chain, the more the solubility of the surfactant is decreased. In contrast, xanthates are highly soluble in water and generally contain 2 to 5 carbon chains [18].

It has been established that the efficiency of separation of metals in solution during ion flotation is based on the use of collectors with the opposite charge to the metal ion to be separated [17]. However, IF is a very versatile process and can be used, including cationic collectors, for the recovery of metal ions, such is the case for silver(I) in solution and other metals, achieving high recoveries, for example, using dodecyl amine and ethanol as a collector and frother agent, respectively [3].

Ionic flotation (IF) has been used for the recovery of numerous metal ions, such as Y(II), Yb(III) [20], As(V), Hg(II), Pb(II), Cd(II), Cr(III) [1], and Ni(II) [21], among others, using cationic collectors for the separation [22]. The main mechanism that takes place during IF is the electrostatic attraction between the collector or surfactant and the metal ion forming a hydrophobic organometallic complex, this has the property of adhering to the bubbles generated in the process, floating up to the surface of the device. form a bed of foam, pour out of the cell, and concentrate relative to the original solution [23].

The flotation process was used for the first time in the concentration of minerals and emerged as a technique for the separation of valuable mineral sulfides from the gangue, and has extended its field of application to different types of industries and applications, such as extractive metallurgy, textile, wastewater treatment among others that require the removal or recovery of metals in the ionic state of residual, or contaminated diluted aqueous solutions [1,14].

The kinetics of ionic flotation is a subject that has generated interest in the world, the zero, first, and second order models have been studied specifically for the zinc (II) ion to ensure that the ion is kept in solution and does not precipitate, deducing that the system behaves as a first-order flotation process [24]. In another study, ionic flotation of various heavy metal ions has been applied using cationic collectors, finding that the selectivity sequence is Mn(II) < Zn(II) < Co(II) < Fe(III) < Cr(III) and Ag(I) < Cd(II) < In(III) [25]. In another work, the competitive ionic flotation of Cu(II), Zn(II), and Cd(II) is evaluated with the use of nonylphenol polyoxyethyl glycol ether as a non-anionic surfactant and β-CD polymers as complexation agents show that the removal of metal decreases with higher molecular mass of β-CD polymers [26].

The efficiency of the ion flotation is a function of chemical conditions, such as the concentration of the collector, frother agent, and pH, mainly, the physical characteristics of the operation of the flotation cell. The superficial velocity of gas Jg (cm/s) Equation (1) and liquid Jl (cm/s) (2) and the properties of the gas–liquid dispersion as the percentage of gas holdup Eg (%) (3), bubble size Db (cm), bubble specific surface area flux Sb (1/s) (4) [2,27,28], and mechanical factors, such as geometry and design of bubble generators in the flotation device, the sparger is considered the heart of flotation [29].

$$Jg = \frac{Qg}{A}(\text{cm/s}) \quad (1)$$

$$Jl = \frac{Ql}{A}(\text{cm/s}) \quad (2)$$

$$E_g = \frac{\Delta D}{\Delta P} * 100(\%) \quad (3)$$

$$Sb = \frac{6Jg}{Db}(\mathrm{cm/s}) \quad (4)$$

where Qg is the gas (air) volumetric flow of (cm^3/s), Ql is the liquid volumetric flow (cm^3/s), A is the area of the device (cm^2), ΔD is the height difference between the two pressure manometers of water (cm) installed on the cell wall, ΔP separation of the manometers in the flotation cell (cm), and Db the bubble diameter which is estimated with the drift flux model [27,28,30–33].

The works mentioned above use batch ion flotation systems and cationic collectors of long hydrocarbon chains, making their solubility in water difficult, for which, in this research, it is proposed to use a continuous ion flotation system using xanthate, dithiophosphate, dithiophosphinates, and polyglycol molecular weight MW 400 ether as collector-promoter and frother, respectively, to recover the silver(I) contained in diluted aqueous solutions of thiosulfate, and to study the kinetics and hydrodynamics of the flotation system in cells with porous spargers.

This research article is novelty compared to what was previously published [2–6]. In this study, the recovery of silver(I) found in form of silver(I) thiosulfate in diluted aqueous solutions is tested. The use of this complex keeps silver(I) in solution due to its range of thermodynamic stability, which is even at alkaline pH values [4].

For this, a flotation system completely different from that reported in the literature [2] is used. The flotation cell can present several advantages with respect to other equipment, these are the decreases in the residence time of the continuous and dispersed phases, and the mixing conditions inside the cell, these allow for the increase of bubble-organometallic contacts to increase the efficiency of separation by flotation and ionic flotation in an aerated cell with spargers allows the system to operate with larger gas flux, increasing the gas holdup, decreasing the bubble size, and thereby, increasing the bubble specific surface area flux.

In addition, alternate reagents are used that have not been previously tested, such as dithiophosphate and dithiophosphinate promoters. as Additionally, a different geometry and a different dispersion and air bubble system than previously reported with respect to the ceramic sparger is tested.

2. Materials and Methods

2.1. Equipment and Materials

The ion flotation tests were performed in a 19 cm × 19 cm by 37.3 cm high acrylic sub-aerated cell, as shown in Figure 1. Inside the equipment, on one of the cell walls opposite to the discharge, two water pressure manometers were installed 17 cm apart and at 6 cm height measured from the base of the cell to measure the hydrostatic pressure and calculate the percentage of v/v of gas holdup.

The feed and discharge (tails) were located 4 cm from the bottom of the cell and placed opposite to each other, both liquid streams were controlled with a pair of Cole Palmer peristaltic pumps with a maximum flow rate of 8 L per minute (lpm) calibrated prior to the flotation tests, calibration is shown in the Supplementary Materials.

The air fed to the cell was controlled with an Omega flowmeter from 0 to 16 L/min, which was passed through two types of porous spargers, a rigid one and a battery of flexible spargers, arranged horizontally at the bottom of the cell, which is a rigid flat ceramic made with shell molding sand (sintered in a mold at 200 °C for two hours), as shown in Figure 2a, the image is a representation of surface porosity of the sparger. The microscopic texture of the surface porosity of the rigid sparger is shown in Figure 2b.

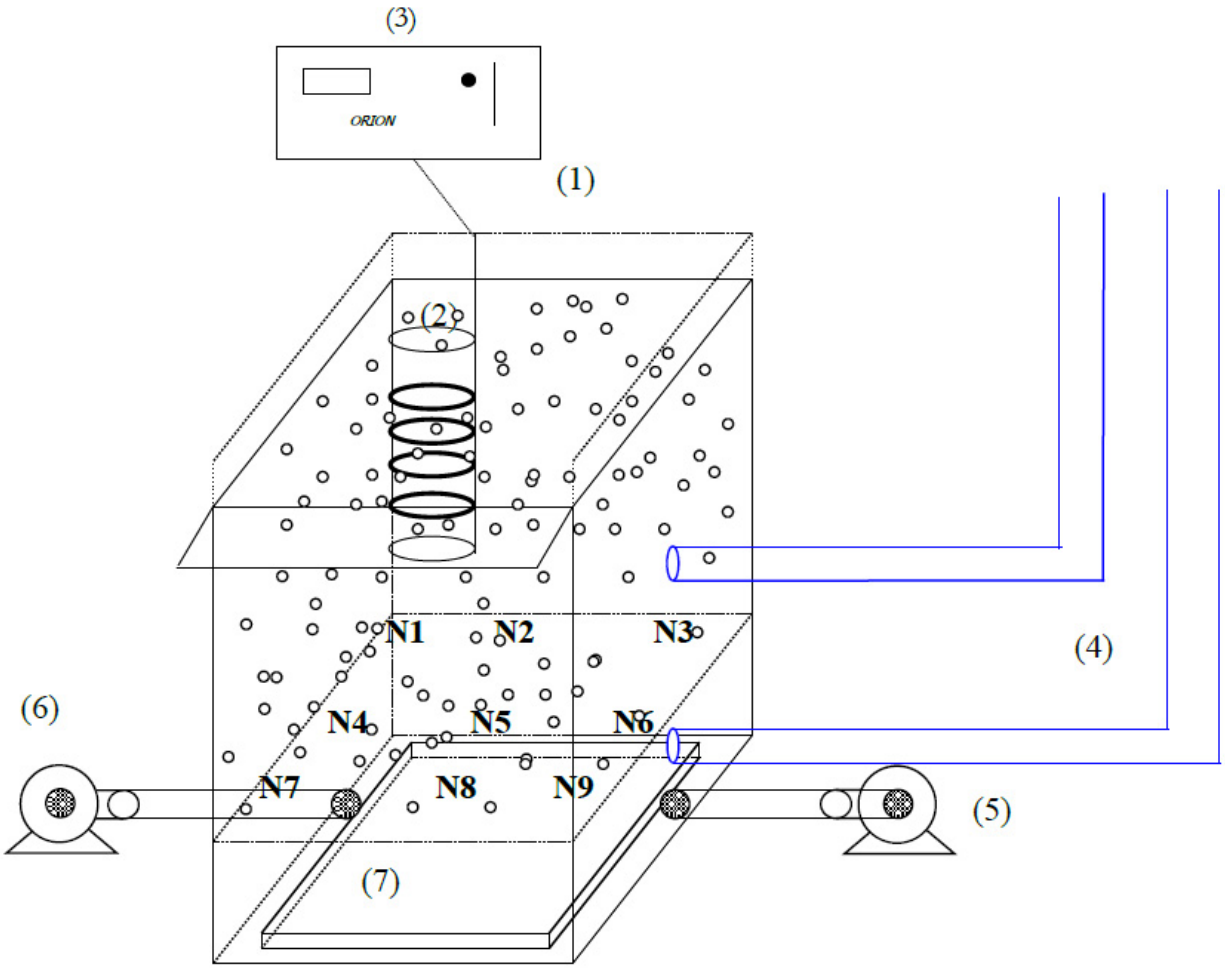

Figure 1. Schematic representation of the flotation device: (1) Cell, (2) Electrical conductivity flow cell, (3) Conductivity meter, (4) Manometers, (5) and (6) Peristaltic pump feed and tailing, respectively, and (7) Flat sparger.

Figure 2c shows the design of the flexible sparger made of PVC sections and covered with several layers of synthetic fabric, as seen in Figure 2d macrograph and micrograph SEM of the porosity of the flexible sparger.

In addition, the gas holdup Eg was estimated using electrical conductivity flow cells described in the literature using Maxwell's model [30–33] constructed of 2.5 cm diameter acrylic cylindrical sections and 4 graphite rings of 1 cm wide, each 2.5 cm apart, as shown in Figure 3A. The electrodes at the ends are of opposite polarity to those in the middle, thus avoiding the outflow of electric current from the interior where the measurements are made to the surroundings. The conductivity flow cell was connected to an Orion model 130 conductivity meter.

The flow cell was calibrated using electrolyte diluted aqueous solutions of different electrical conductivity by dissolving certain amounts of 99% pure potassium chloride (KCl) in water to give various liquid conductivities. The purpose of this calibration is to know the electrical cell constant, and thus convert the conductance values read with the flow cell to electrical conductivity and use them in Equation (5).

$$Eg = \frac{1 - \left[\frac{kd}{kl}\right]}{1 + \left[0.5 * \frac{kd}{kl}\right]} * 100 \quad (5)$$

where kd is the conductivity of the dispersion (gas-liquid), kl is the conductivity of the liquid only, and Eg is the gas holdup expressed as a percentage. Once the cell constant Figure 3B is known, it can be used to estimate the electrical conductivity from conductance measurements made with the flow cell inside the flotation cell.

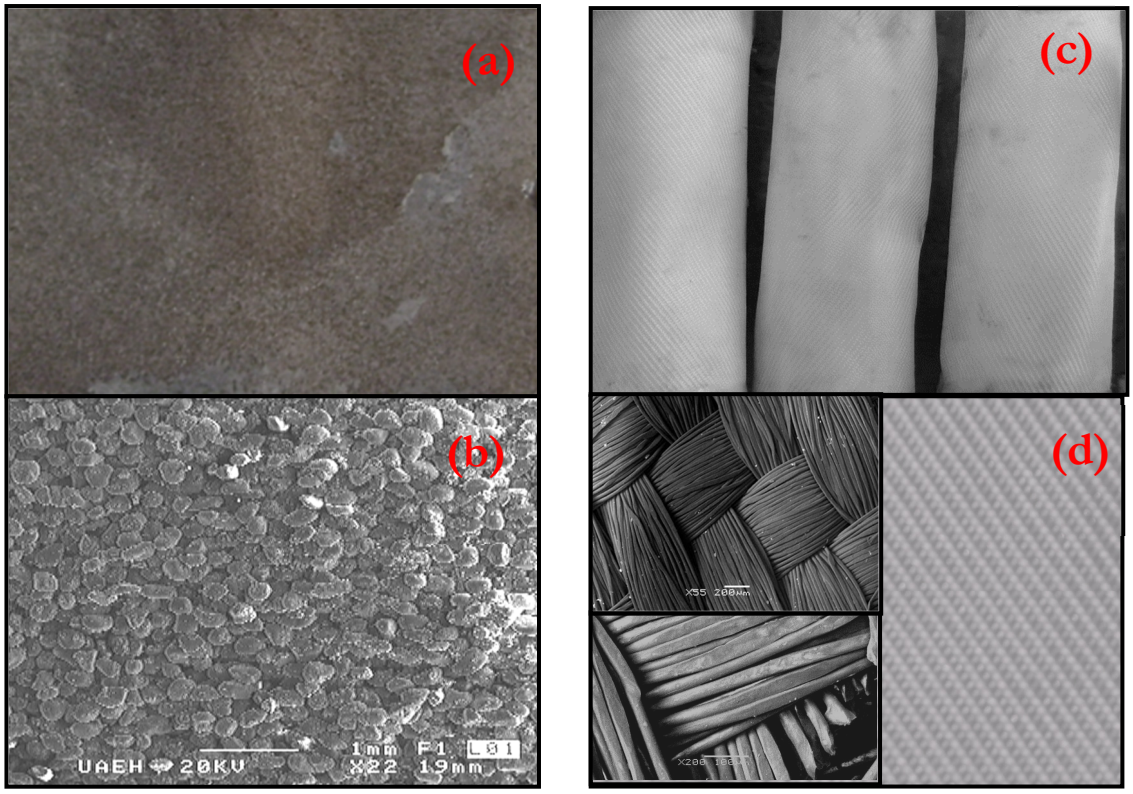

Figure 2. (**a**) Appearance of the flat sparger, and (**b**) micrography of the surface porosity; (**c**) appearance of the battery of cylindrical spargers, and (**d**) texture of the superficial porosity of the synthetic fabric.

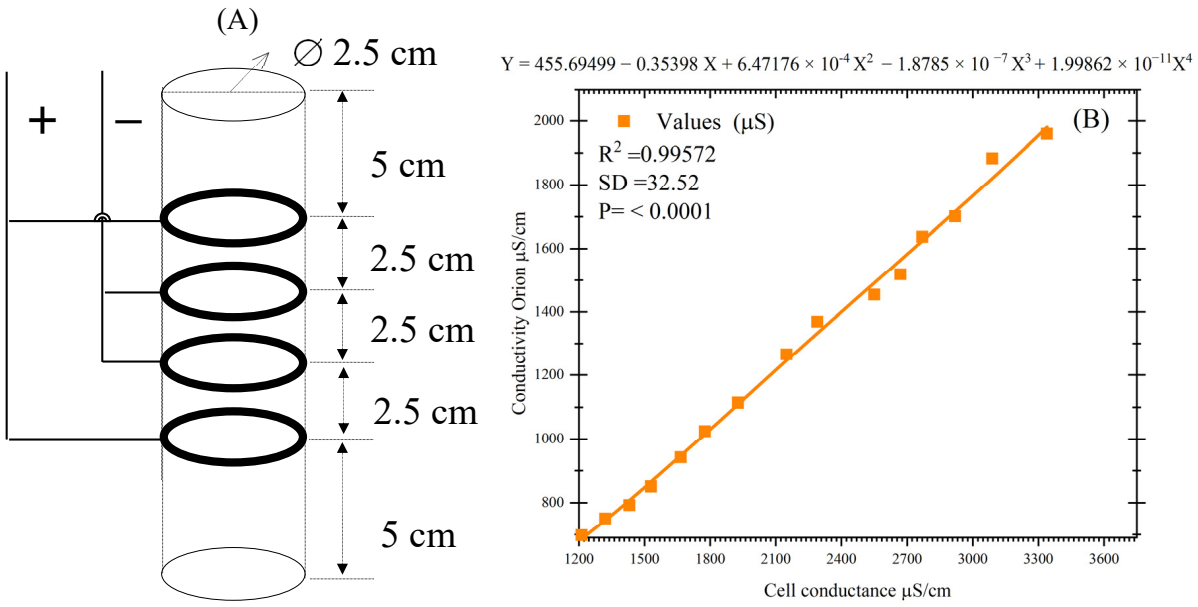

Figure 3. (**A**) Schematic representation of the conductivity flow cell with 1 cm thick graphite electrodes, and (**B**) electrical conductivity flow cell calibration curve.

2.2. Experimental Procedure

The ion flotation tests were carried out in a single stage with continuous recirculation of the solution (20 L) containing 3.52×10^{-4} of silver(I) in the form of diluted aqueous solutions of silver(I) thiosulfate $Ag[S_2O_3]_2^{-3}$ Log K = 13.4 [34], the feed and discharge to the flotation cell was carried out at a superficial liquid velocity Jl of 0. 20 and 0.19 cm/s, respectively, a frother concentration [e] of 1.25×10^{-4} of poly glycol ether with a molecular weight 400 was added. In each chemical and physical modification to the flotation system, a conditioning time of 5 min was given to allow the homogenization of the phases.

After the frother agent, the collector sodium isopropyl xanthate $C_4H_7NaOS_2$ (XIS) is added at concentrations of 1.26, 2.52, 3.15, and 3.77×10^{-4} M, respectively. In separate tests, the effect of the xanthate–dithiophosphate and dithiophosphinate combination, the concentration of the frother, the pH, and the geometry of the bubble dispersion system, and their influence on the silver(I) recovery from the solution were analyzed.

During the experimentation, once the chemical conditions of the continuous medium (liquid or solution) were established, air was injected through the porous dispersers using superficial gas velocity Jg from 0.1 to 1.0 cm/s. The volumetric air flow rates as a function of the Jg used are shown in the Supplementary Materials.

At each Jg increment, the height of the foam bed (hfb) in the flotation cell was measured and before starting the silver(I) recovery and sampling the liquid streams (feed, tails, and concentrate), an interval of twice the residence time (τ) was given as in Equation (6). Once concluded, the concentrate, tails, and feed streams were sampled; the sampling time was taken; and the collected sample was weighed to carry out a mass balance of the silver(I) separation as a function of the superficial gas velocity and the gas holdup.

$$\tau = \frac{hcz - hfb}{Jl} * (1 - Eg) \quad (6)$$

where hcz is the height of the collection zone in cm, hfb is the height of the foam bed in cm, Eg is the fraction of gas holdup, (1 − Eg) is the fraction of liquid holdup, and Jl is the superficial liquid velocity cm/s. The samples collected from the three flotation streams were diluted and analyzed in an atomic absorption spectrometer (Perkin Elmer 3100) and the percentage recovery was obtained with Equation (7).

$$\%R = \frac{[FMc]}{[FMc] + [FMt]} * 100 \quad (7)$$

where FMc is the mass flow rate of the concentrate, FMt is the mass flow rate of the discharge (tails) in unit's grams of silver(I)/minute.

During all the flotation tests, the gas holdup from the dispersion was estimated with two methods, one global and the other local, the first by pressure differences (ΔD) in a section within the collection zone below the foam bed. It should be noted that in the manometric method an average value of the gas volume contained between the two pressure taps is obtained, which gives margin for errors if the gas is not homogeneously distributed in the flotation cell.

On the other hand, the local method consists of placing the electrical conductivity flow cell in nine different positions throughout the cross section of the flotation cell and measuring the conductance of the dispersion and that of the liquid to determine the Eg locally.

Regarding the flotation kinetic constant, it was obtained with Equation (8), for a cell with a perfect mixing behavior, where the residence time distribution is the same in all the equipment, this equation is applied when there is a constant homogeneous and uniform flux of bubble size characterized by a linear relationship in the superficial gas velocity vs. gas holdup graph [18,27].

$$R = 1 - (1 + k * \tau)^{-1} \quad (8)$$

3. Results and Discussion

3.1. Flotation Cell Hydrodynamic Characterization

Prior to the silver(I) ion flotation tests, the dispersion system was hydrodynamically characterized by analyzing the behavior of percentage of v/v gas holdup (Eg), bubble diameter Db (cm), and bubble specific surface area flux Sb (1/s) (cm^2 bubble surfaces/s)/(cm^2 cell area) as a function of superficial gas velocity Jg (cm/s) in systems with only frother agent for the flat bubble generator constructed of ceramic material with molding sand.

Figure 4 shows the percentage of v/v Eg estimated with the pressure manometers, as a function of Jg in a range from 0.1 to 1.5 (cm/s) and a superficial liquid velocity Jl in the discharge of 0.19 cm/s without and with 0, 2.5×10^{-5}, 7.5×10^{-5} and 12.5×10^{-5} M frother agent. The percentage of Eg in the cell increases with Jg and [e], obtaining similar values of Eg for Jg between 0.1 and 0.8 cm/s. Moreover, the linear behavior of the percentage of v/v Eg Vs Jg changes from Jg of 0.8 cm/s onwards. The maximum percentage of v/v Eg with a Jg of 1.5 cm/s was 13.5%, 20.5%, and 28.2% for the [e] of 2.5×10^{-5}, 7.5×10^{-5}, and 12.5×10^{-5} M, respectively.

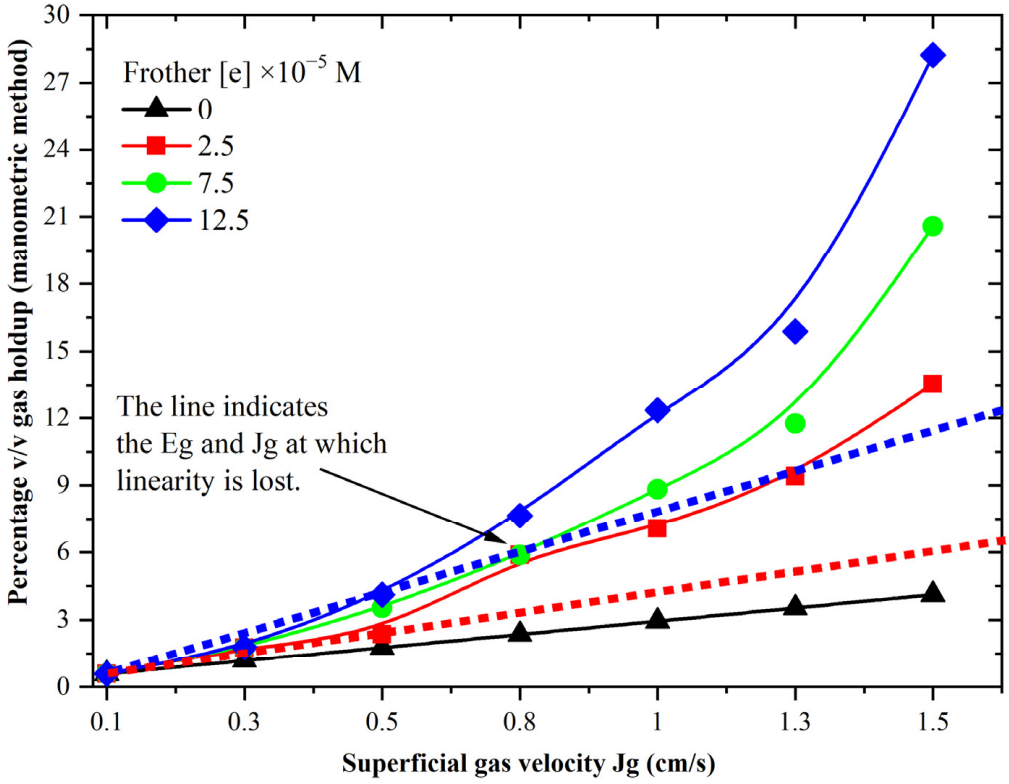

Figure 4. Percentage of v/v gas holdup as function of superficial gas velocity Jg (cm/s), Jl 0.19 cm/s, [e] 0, 2.5, 7.5, 12.5×10^{-5} M, rigid sparger.

The change of linearity in the Eg Vs Jg graph is interpreted as the transition from a homogeneous liquid and bubble flux regime to a turbulent one in which an increase in bubble recirculation is generated, increasing their residence time inside the flotation cell and therefore of the Eg, generating zones of different relative densities due to the effect of the increase in the gas holdup causing higher circulation currents and mixing of the liquid and gas phases.

The percentage of v/v Eg was further estimated using electrical conductivity flow cells, and the measurements were performed at 9 different positions within the collection zone of the flotation cell. Figure 5 shows the comparison of the gas holdup obtained by the two methods, manometric and electrical conductivity. Similar to what is shown in Figure 4, the linear behavior between the percentage of v/v Eg and Jg is modified from Jg 0.8 cm/s onwards.

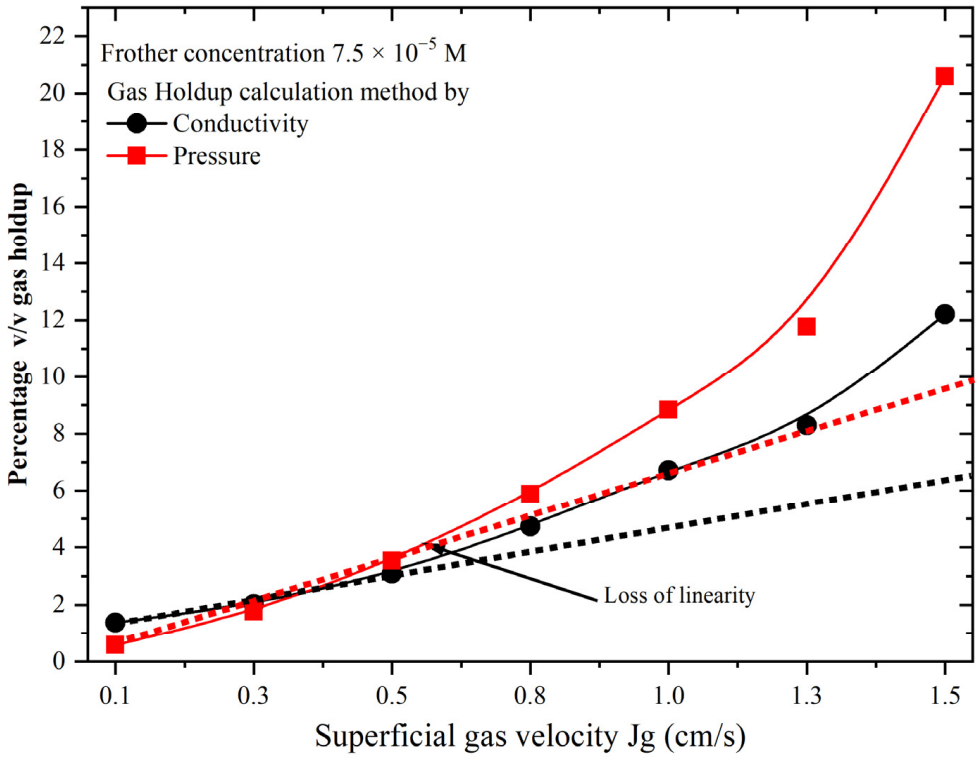

Figure 5. Percentage of v/v gas holdup as function of superficial gas velocity Jg (cm/s), Jl 0.19 cm/s, [e] 7.5 × 10^{-5} M, rigid sparger. Percentage of v/v Eg Differentiation by pressure and conductivity. The red and black dotted lines indicate the loss of linearity.

The gas holdup measured by manometric pressure presents higher values with respect to the conductivity method because they are global values and depend on the distribution of bubbles in the flotation cell, while by the conductivity method the percentage of v/v Eg depends on the punctual measurements of electrical conductivity made with the conductivity meter. These differences found in the percentage of v/v Eg are also attributed to the bubble size distribution in the flotation cell.

From the point sampling in nine different zones in the flotation cell for the estimation of the percentage of v/v Eg, it was determined that the increase in Jg generates greater mixing intensity, bubble recirculation, sections where the gas holdup is greater, and places where there is a homogeneous flux of bubble surfaces.

Figure 6 shows the distribution of the percentage of v/v of Eg in the flotation cell, the zones with higher gas holdup are those with lower relative density due to the lower amount of liquid and a dense cloud of recirculated bubbles that cause the gas holdup to increase, these differences occur mainly when the Jg is 0.8 cm/s or higher due to the effect of the mixing currents the bubble flux recirculates inside the cell, they concentrate in the central part and eventually leave the flotation cell.

The recirculation streams preferentially entrain the smaller bubbles, increasing their residence time, and thus the gas holdup. The bubble diameter was estimated with the drift flux model using the superficial gas velocity, liquid, the fraction of gas holdup, Reynolds number, and data on the density and viscosity of the continuous medium, the procedure is described in the literature [27,35–37] and in the Supplementary Materials.

Figure 7 shows the bubble diameter Db (cm) as a function of Jg (cm/s) for different [e], Db decreases with Jg and with the concentration of frother, it is expected that with the decrease in bubble size, the bubble specific surface area flux available to carry out the separation process increases; however, the optimum Db must be found because smaller bubbles tend to be dragged by the circulation and mixing currents increasing their residence time and decreasing the separation of the phases of interest.

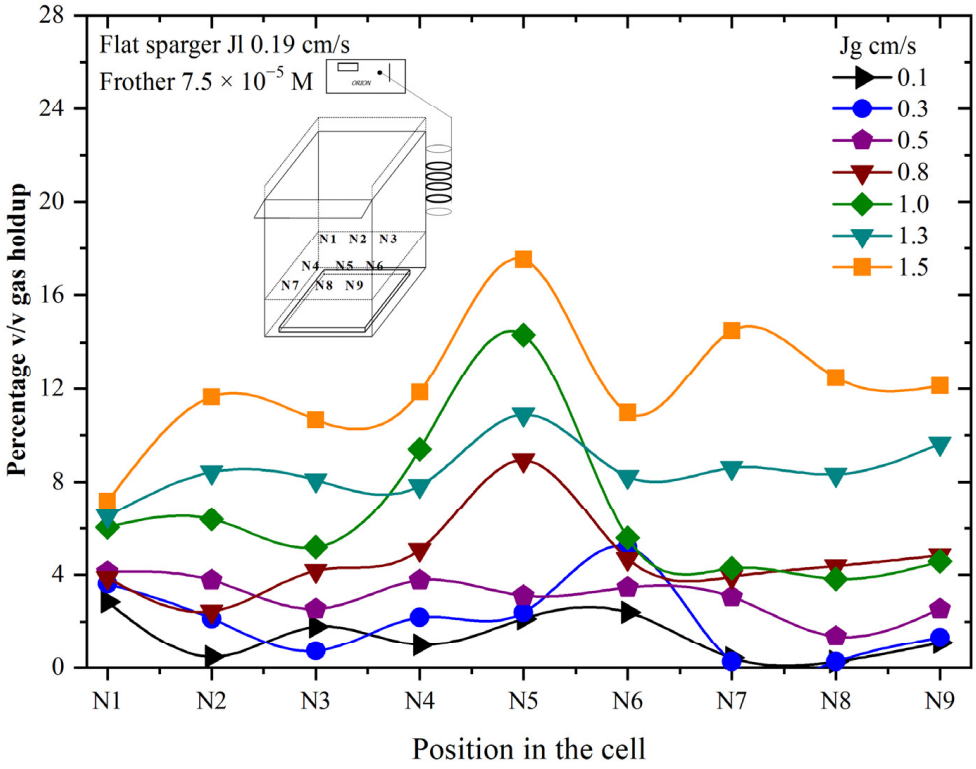

Figure 6. Percentage of v/v gas holdup distribution in the cell flotation, [e] 7.5 × 10^{-5} M, Jl 0.19 cm/s, Jg 0.1 to 1.5 cm/s.

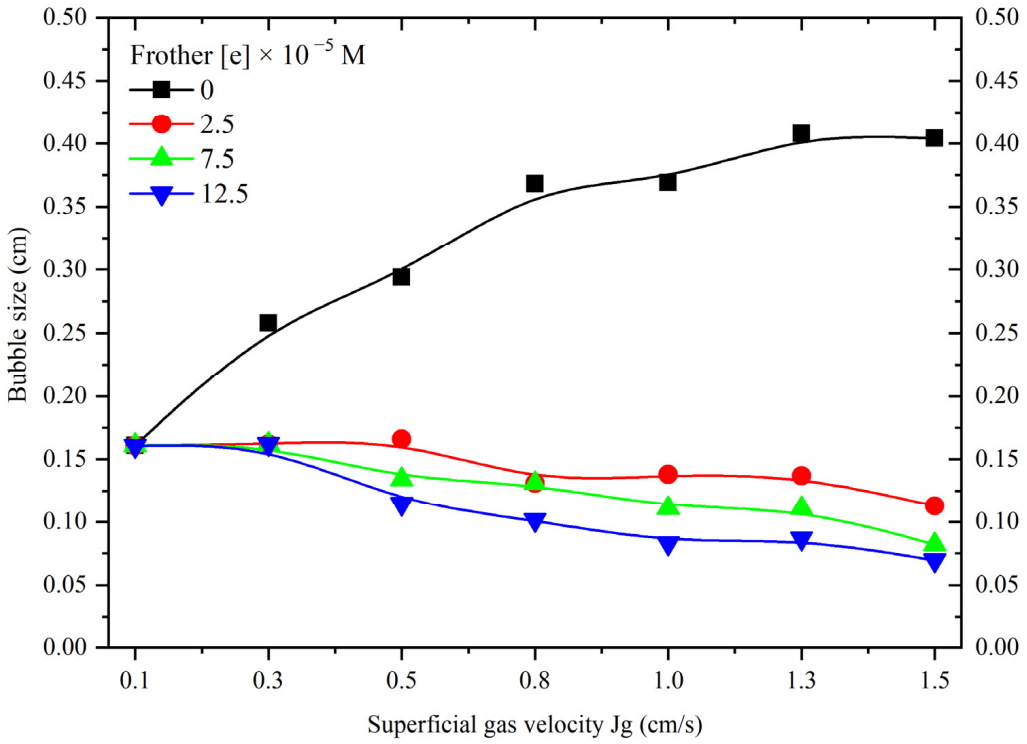

Figure 7. Bubble diameter (cm) as function of superficial gas velocity Jg (cm/s), [e] 0, 2.5 × 10^{-5} M, 7.5 × 10^{-5} M, and 12.5 × 10^{-5} M, ceramic sparger.

As shown previously in Figure 6, the distribution of percentage of v/v Eg is not uniform in the flotation cell, which indicates the existence of high and low relative density zones, and therefore, variations in bubble size generate the circulation and mixing currents.

Furthermore, with the decreasing bubble size, it is expected that the bubble specific surface area flux Sb (1/s) will increase as represented by Equation (4) shown above.

With the bubble diameter and superficial gas velocity Jg, it is possible to obtain the value of Sb (s-1). This is considered an important parameter in flotation processes as it adequately represents the machine factors with the Jg indicating the aeration ability of the cell, and the chemical factors with the gas dispersion efficiency using the bubble diameter; however, in extractive metallurgy, it is preferable to look at the bubble diameter as a reference to the separation efficiency.

3.2. Ion Silver(I) Flotation

During the binding process of silver(I) ions with organic xanthate molecules, the mechanism of xanthate oxidation occurs and is magnified by the increase in the concentration of dissolved oxygen caused by the aeration of the cell forming di xanthate [35]. The oxidation potential E° (V) of xanthates increases with the number of carbons in the hydrocarbon chain; for this study, sodium isopropyl xanthate (SIX) with a potential of—0.068 V was used.

The solubilization and oxidation of xanthate in water forms di xanthate ion and sodium ion, the aqueous xanthate molecule attracts aqueous metal ions of opposite charge to the valence of the sulfur radical by electrostatic and Van Der Waals attraction. The reaction mechanism of xanthate (SIX) with silver(I) is as follows:

$$2Ag^{+} + 2[C_4H_8OS_2]^{-} = 2Ag[C_4H_8OS_2]_{aq} \quad (9)$$

The process of capturing silver(I) ions during ion flotation is mainly due to electrostatic attractions between the inactive surface ion Ag(I) and the negatively charged collector, forming a hydrophobic aqueous silver(I) complex, which adheres to the air bubbles generated in the flotation cell, floats to the surface, and concentrates with respect to the original solution. Xanthate is one of the most widely used reagents in industrial flotation circuits because it is biodegradable at low concentrations, water soluble, and inexpensive [18].

3.2.1. Effect of the Collector Concentration

Figure 8 shows the results found for silver(I) extraction by ion flotation using xanthate [x] concentrations of 1.26×10^{-4}, 2.52×10^{-4}, 3.15×10^{-4}, and 3.77×10^{-4} M SIX, Jl of 0.19 cm/s, respectively, this is a function of the superficial gas velocity. For concentrations of 1.26×10^{-4} and 2.52×10^{-4} M of [x], the silver(I) recovery increases with Jg obtaining a maximum extraction of about 70% with Jg values of 0.5 cm/s, the increase in Jg leads to the decrease in silver(I) separation.

This drop in recovery is attributed to what is described in the hydrodynamic characterization of the flotation cell, in which the loss of linearity of Eg Vs Jg behavior modifies the bubble flux regime from homogeneous to turbulent, causing circulation currents and bubble mixing inside the cell, decreasing the flotation kinetics due to the increase in the residence time [38] of the bubbles with the collected silver(I)-xanthate organometallics, and the coalescence of bubbles and release of the collected species can occur.

With increasing Jg the amount of gas holdup in the flotation cell is also greater, the bubble diameter decreases and a relatively larger bubble specific surface area available to separate the species of interest overlaying the turbulent mixing currents, which happens for silver(I) extraction at a xanthate concentration of 1.26×10^{-4} M and at Jg of 1.0 cm/s, where the percentage of w/w silver(I) recovery by ion flotation increases, as shown in Figure 8

The optimum concentration for the best silver(I) recovery was at 3.77×10^{-4} M of XIS, Jg at 0.3 and 0.5 cm/s, respectively, and Jl at 0.19 cm/s with maximum extraction of 90% silver(I). Higher Jg does not contribute to increasing the separation efficiency, due to the turbulence conditions generated which causes the bubbles with the collected species to remain inside the cell longer and eventually spill out of the cell.

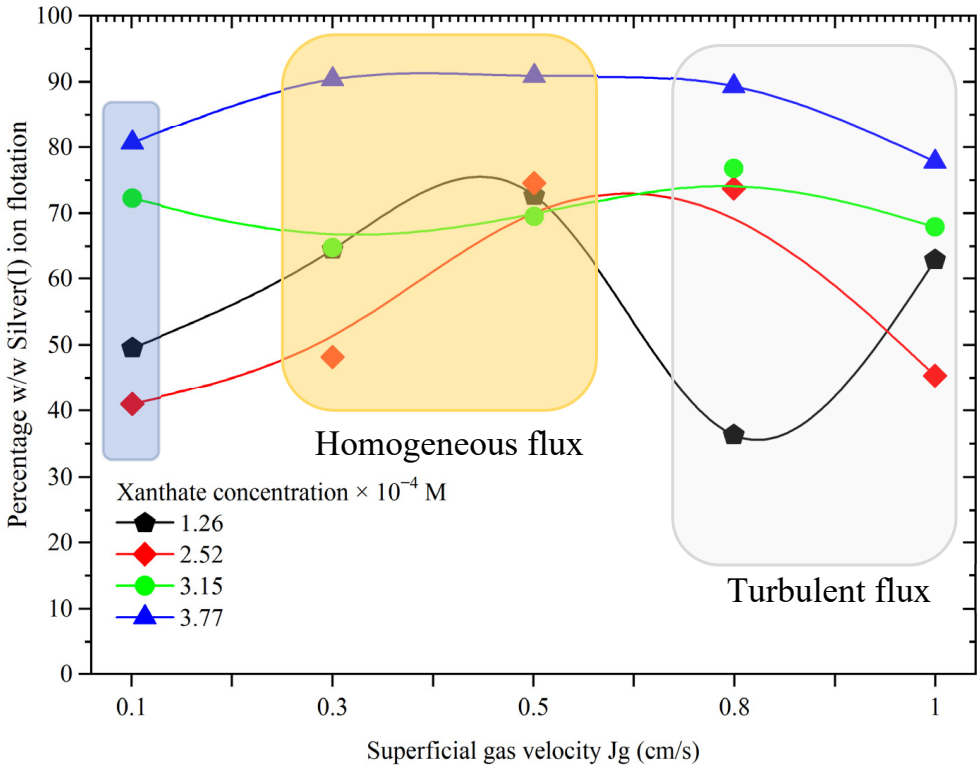

Figure 8. Percentage of w/w of silver(I) ion flotation as function of superficial gas velocity, ceramic sparger, Jl 0.19 cm/s, and [e] 1.26, 2.52, 3.15 y 3.77 × 10^{-4} M of xanthate.

The silver(I) recovery system by ion flotation of each of the tests performed, the calculation of the percentage of gas holdup, the bubble diameter with the drift flux model [35–37,39], the bubble specific surface area flux, and the flotation kinetic constant were applied to the silver(I) recovery system. The species collection process in a sub-aerated flotation unit is a first-order kinetic process, with a collection rate constant (k) (1/min) [27,38].

It is established that the recovery of a species is a first order process and depends on three parameters: the rate constant, the mean residence time, and the mixing parameters. Therefore, the mixing conditions must be known (piston-type flux pattern or perfect mixer model) before estimating the flotation kinetic constant [27,38].

In the flotation cell, the perfect mixing model is used with a residence time τ and the flotation kinetic constant, given by Equation (8), is obtained as shown in Equation (10) [27].

$$k = \frac{R}{(1 - R) * \tau} \tag{10}$$

where k is the kinetic constant of flotation, (τ) is the apparent residence time, and R is the recovery of the species in (fraction). The flotation constant is related to Jg and Db; therefore, the necessary condition to maintain the kinetic constant in the scaling is to have the same bubble diameter at the same superficial gas velocity from the laboratory experiments. Therefore, k is independent of the diameter and size of the flotation equipment used [27,38].

Figure 9 shows the percentage of w/w silver(I) ion flotation, percentage of v/v Eg, the Db, and Sb, as a function of the superficial gas velocity Jg (cm/s) for the silver(I) recovery test by ion flotation in the presence of 3.77 × 10^{-4} M of SIX. The increase in the percentage of v/v of Eg as a function of Jg (cm/s) is highlighted, while the bubble diameter tends to decrease, being the optimum size of 0.11 cm, in which the highest silver(I) extraction occurs with the decrease in Db and an increase in the silver(I) extraction would be expected due to the increase in the bubble specific surface area flux; however, the extraction decreases

due to the longer residence time of the dispersed phase in the flotation cell. The flotation kinetic constant obtained from the best recovery is 4.16 1/min.

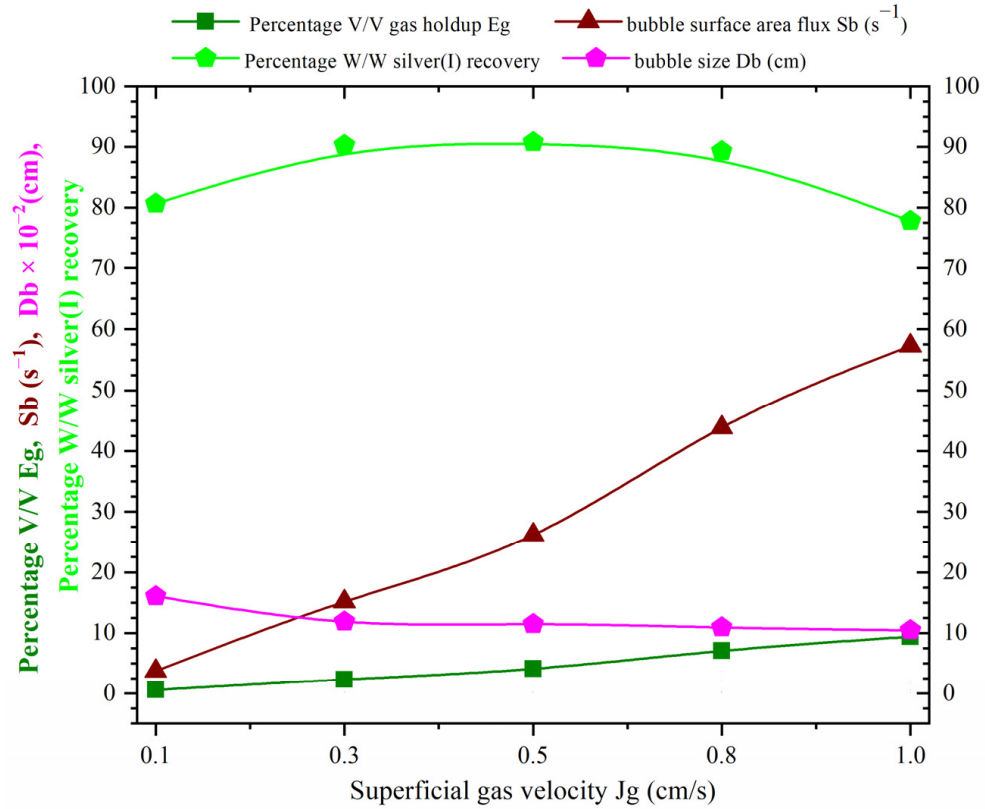

Figure 9. Eg, Db, Sb, and percentage of w/w of silver(I) ion flotation as a function of superficial gas velocity, ceramic sparger, Jl 0.19 cm/s, [e] 1.25 × 10^{-4} M, and xanthate concentration 3.77 × 10^{-4} M.

Ion flotation in cells with porous ceramic spargers show shorter residence times of both the dispersed phase (gas holdup) and the continuous phase (liquid) compared to a column flotation system, which the latter presents a change of bubble flux regime from homogeneous and stable to turbulent at a Jg of 0.3 cm/s, while, in a cell-type flotation equipment with porous spargers, the loss of linearity of the graph percentage of v/v of gas holdup (Eg) as function of superficial gas velocity Jg is lost at 0.8 cm/s [2].

Therefore, in the case of the flotation column, the turbulent bubble flux regime at small Jg (0.3 cm/s) causes the recirculation of bubbles, especially those of smaller diameter, which leads to an increase in gas holdup, as reported in previous works. These characteristics will lead to a decrease in the bubble size, increasing the bubble specific surface area flux Sb (cm^2 bubble surfaces/s)/(cm^2 column area) available for separation. However, the time that the bubbles spend inside the column is greater due to the effect of the circulation and mixing currents where these bubbles eventually come out from the column and concentrate on the desired species [2].

The recirculation of bubbles in the flotation column leads to the increase in the gas holdup, which compared to the flotation cell is higher. For example, the gas holdup where the separation efficiency is higher in the column at Jg 0.5 cm/s is of around 11.7% v/v Eg, while in the cell at the same value of Jg it is 4.1% v/v Eg and the silver(I) separation efficiencies are 95% and 90% w/w, respectively, under these conditions there is a residence of 7.3 min for the flotation column, while for the cell it is 2.35 min. These are the main differences between using a column of or a flotation cell [2].

3.2.2. Collector—Promoter Effect

It has been cited in the literature that the use of a promoter reagent together with xanthate improves the recovery process [18]. Figure 10 shows the percentage of w/w silver(I) extraction by ion flotation as a function of Jg for combinations of xanthate 1.57×10^{-4} [x]—0.82×10^{-4} [xl245] Di thiophosphate, 1.57×10^{-4} [x]–1.08×10^{-4} [xl2945] dithiophosphinate and the use of only promoters, reagents supplied by Alkemin S.A. de S.R.L.

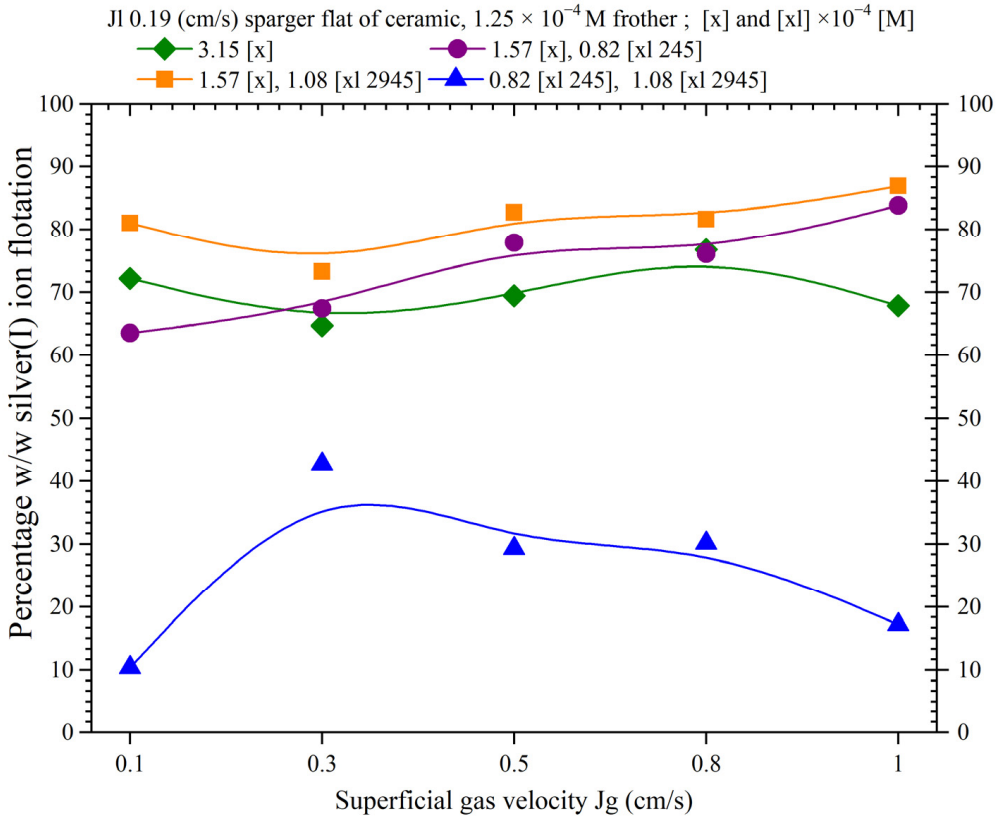

Figure 10. Percentage of w/w silver(I) recovery by ion flotation as function of superficial gas velocity, collector–promoter and promoter combinations Jl 0.19 cm/s, ceramic sparger flat.

The use of these combinations improves the extraction compared to the system using only xanthate. Using 1.57×10^{-4} M of [x] and 1.08×10^{-4} M of [xl2945] allows us to obtain the best recoveries, which was 86.9% w/w of Ag recovery at Jg 1.0 cm/s; however, this does not exceed that obtained in the test using 3.77×10^{-4} M of [x] shown in Figure 9.

Furthermore, the recovery using a [x]–[xl245] combination is higher than that of the system with only [x], while in the system using only [xl245]–[xl2945] combinations, it is not recommended due to the low silver(I) extractions, which, in the best case at Jg of 0.3 cm/s, is 42% w/w higher, and gas surface velocities do not contribute to the improvement of the recovery, including decreases.

The analysis of the relationship of the dispersion properties Eg, Db, Sb, and silver(I) recovery for the system using 1.57×10^{-4} [x]–1.08×10^{-4} [xl2945] as a function of Jg is presented in Figure 11. The use of this combination improves the hydrodynamic conditions of the cell and can operate with significant efficiencies up to Jg values of 1.0 cm/s, at which the best silver(I) extraction is obtained, being the maximum Eg percentage of v/v of 11.17%, with an average bubble diameter of 0.86 cm; this Db, compared to the system with only xanthate shown in Figure 8, is slightly lower.

The use of promoters to the flotation system provides greater hydrodynamic stability to the dispersion system. With the decrease in Db (cm), the amount of bubble specific surface area flux Sb (1/s) available to perform the separation increases compared to the tests with only xanthate at Jg of 1.0 cm/s and Sb of 66.58 (1/s). These properties of the

dispersion and hydrodynamics of the flotation system allow us to obtain the maximum extraction a flotation kinetics of 3.6 1/min.

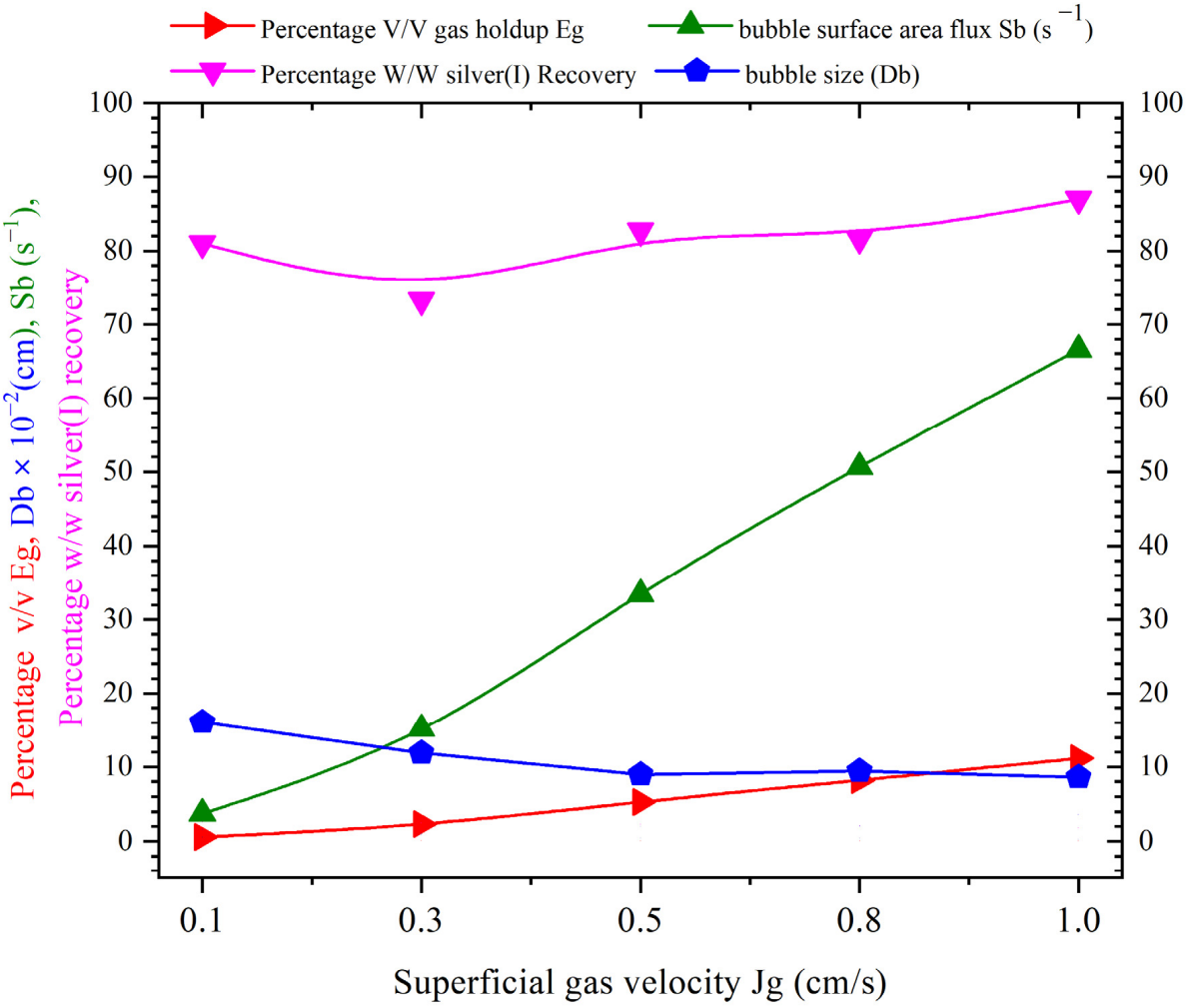

Figure 11. Eg, Db, Sb, and percentage of w/w of silver(I) ion flotation as function of superficial gas velocity, ceramic sparger, Jl 0.19 cm/s, system 1.57 × 10^{-4} of [x]—1.08 × 10^{-4} [xl2945], and [e] 1.25 × 10^{-4}.

The chemistry of the flotation system performs a preponderant role in the recovery of silver(I) by ion flotation, which was found for the tests by using combinations of 0.82 × 10^{-4} L [xl245] and 1.08 × 10^{-4} [xl2945]. Despite the favorable hydrodynamic conditions represented by the percentage of v/v graph of Eg vs. Jg (cm/s), which shows a linear behavior in Figure 12A, i.e., a stable and homogeneous bubble flux in the whole range of Jg studied, the separation efficiency is very low (42% w/w separation).

Regarding the hydrodynamics of the system, Figure 12B shows the behavior of the properties of the gas dispersion, where the percentage of v/v of Eg increases with the Jg, being a maximum of 11.1%, the Db decreases, and an optimum size of 0.9 cm is achieved. Regarding the Sb, this increases with the decrease in the Db and a value of 66. 5 (1/s). Despite the favorable machine conditions to carry out the ion flotation of silver(I), the recoveries are low, for example, at Jg 1.0 cm/s are 17% w/w, this leads to the obtainment of a kinetic constant of flotation of 0.1 (1/min).

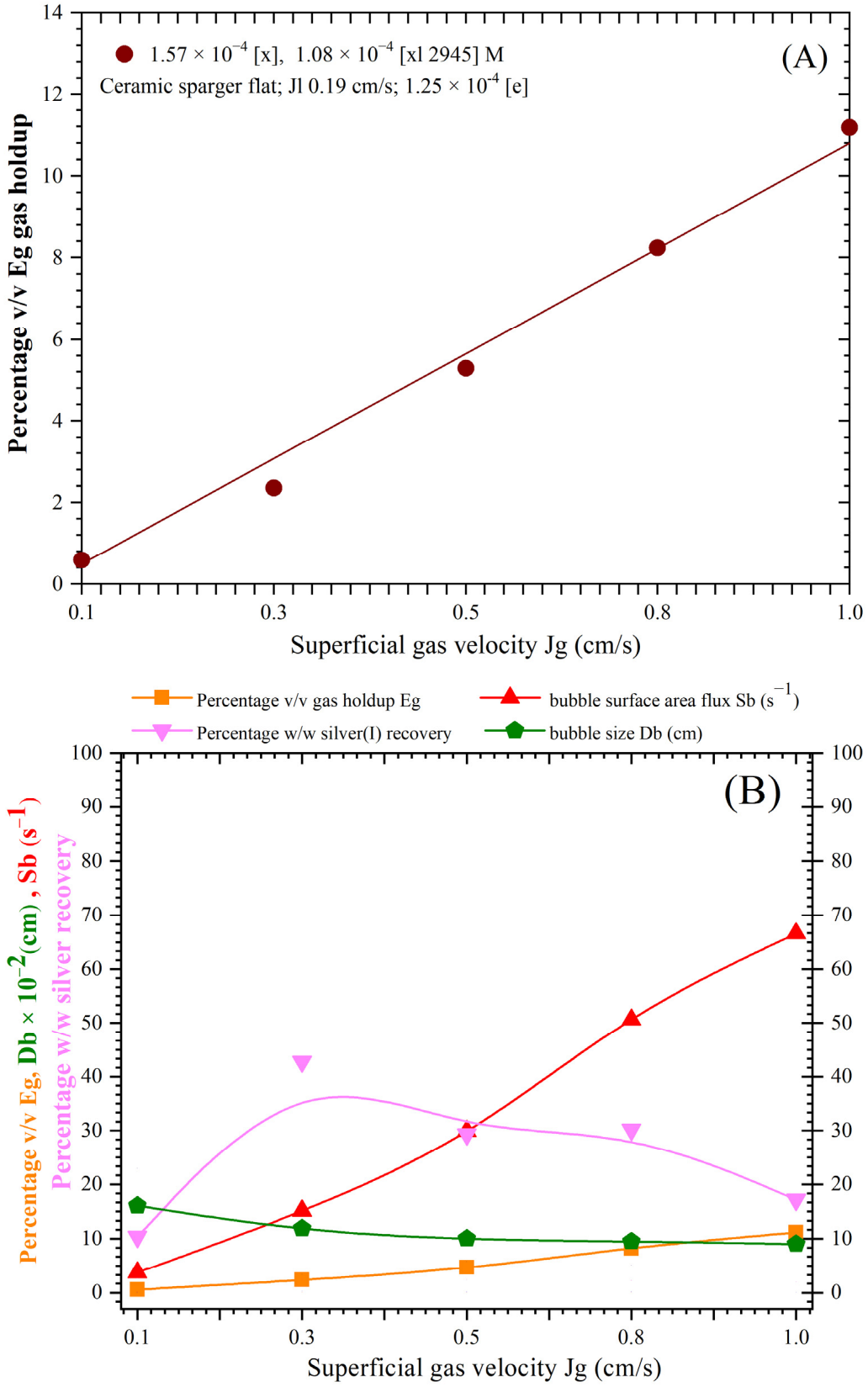

Figure 12. (**A**) Percentage of v/v gas holdup as function of Jg (cm/s). (**B**) Eg, Db, Sb, percentage of w/w of silver(I) ion flotation vs. Jg, ceramic sparger, Jl 0.19 cm/s, and 0.82 × 10^{-4} M [xl245]–1.08 × 10^{-4} M [xl2945].

3.2.3. pH Effect

The percentage of w/w silver(I) extraction is affected by the hydrodynamics of the air–liquid dispersion and to a greater degree by the chemistry of the system, which is affected by the presence of xanthates, xanthate-promoter combinations, and aqueous media containing only promoters and frother, and it is in greater intensity for the latter. Another important factor to evaluate during ion flotation is pH. In the tests presented above, it was observed that the pH of the solution tends to increase with time and with Jg due to the oxidation of xanthate to di xanthogen Equation (11) by the effect of aeration in the cell, this reaction is essential before the xanthates can act as a collector [18].

$$2ROCS_2^- = (ROCS_2)_2 + 2e^- \quad (11)$$

The pH was kept constant during the whole test at 6.0, 7.0, and 8.0, respectively. Depending on the case, the pH was regulated with sulfuric acid or sodium hydroxide, with the pH stable, the test began with maintaining the initial value during the whole time of the test. The results obtained are presented in Figure 13 using a rigid sparger made of ceramic, 1.89×10^{-4} M of xanthate and 1.29×10^{-4} M of promoter xl-2945 dithiophosphinate, and 1.25×10^{-4} M of the frother agent with a Jl of 0.19 cm/s.

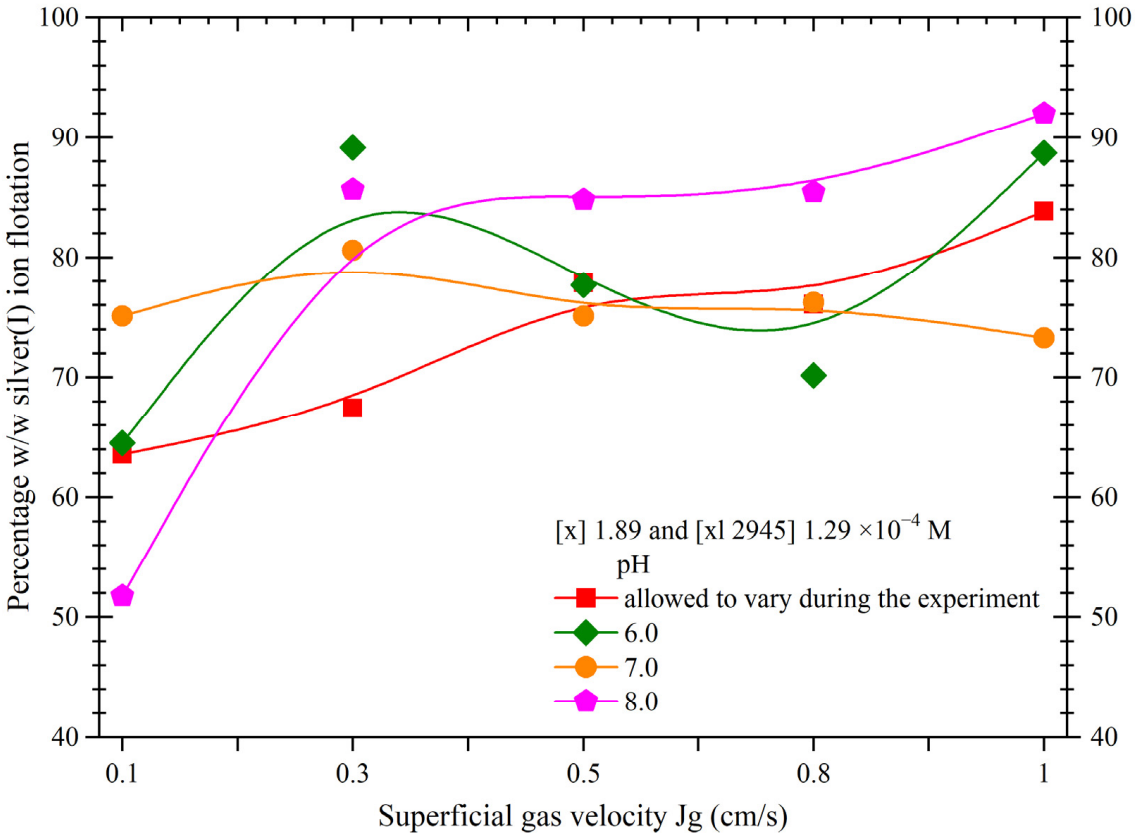

Figure 13. Percentage of w/w silver(I) recovery by ion flotation as function of superficial gas velocity, collector–promoter and promoter combinations Jl 0.19 cm/s, ceramic sparger flat.

The best separation efficiencies are obtained at pH 8.0, when the Jg is 1.0 cm/s obtaining a value of 92% w/w silver(I) ion flotation, while the percentage of v/v of Eg is 8.2%, the average bubble diameter was 0.11 cm, with a bubble surface area flux of 50.5 (1/s), the flotation kinetic constant is 5.3 (1/min), as can be seen in Figure 14.

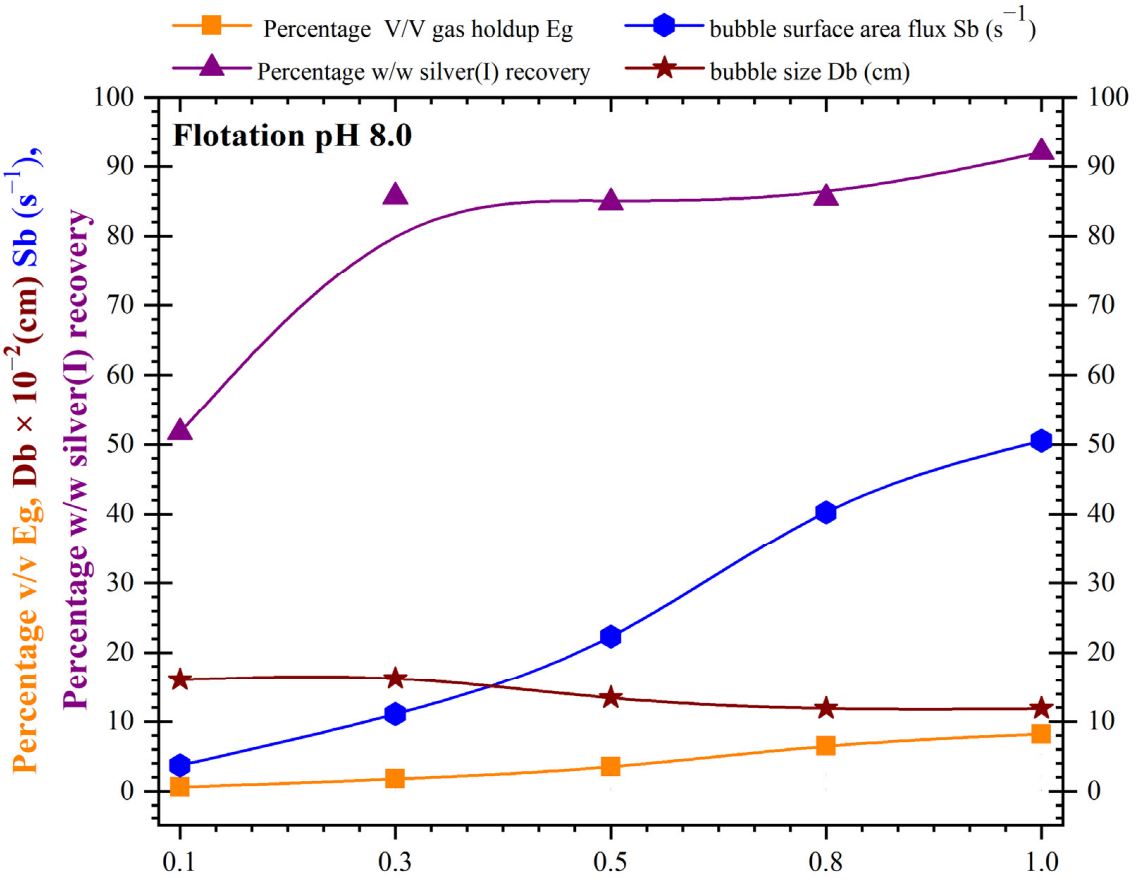

Figure 14. Eg, Db, Sb, and % *w*/*w* of silver(I) ion flotation as a function of superficial gas velocity, ceramic sparger, Jl 0.19 cm/s, system 1.89 × 10^{-4} [x]–1.29 × 10^{-4} [xl2945] M, and pH 8.

Ion flotation is a technique that can be carried out in a wide variety of separation equipment. The difference between one and the other is the hydrodynamic characteristics of the flotation system, which will provide, to a lesser or greater degree, the interaction or contact between the bubble and the species to be separated. In this case, the circulation and mixing currents perform a decisive role in the efficiency of recovery or removal of the metal ion from the solution.

In comparison with the ion flotation system in cells with dispersers, with respect to the separation applied in a column, the latter presents a different behavior, such as the transition from a homogeneous bubble flux regime to a turbulent one at Jg of 0.3 cm/s [2], which is lower with respect to the cell where this change occurs at Jg of 0.8 cm/s. For the flotation column, due to the turbulence, mixing, and recirculation of the continuous and dispersed phases, the gas holdup is greater than that obtained in the flotation cell; therefore, it is expected that the bubble diameter will be smaller, and a larger area bubble surface available to carry out the process in a flotation column. This causes the percentage of *w*/*w* of silver(I) flotation to be 95%, while, for a flotation cell under similar Jg conditions, the efficiency was 90% *w*/*w* [2].

Interestingly, the control of the pH of the flotation solution at pH 8.0 significantly modifies the properties of the dispersion with respect to the change from homogeneous to turbulent flux regime is presented from 0. 8 cm/s as in the previous effects studied. However, in this case, the deviation from linearity is in a greater proportion affecting the hydrodynamics of the system, mainly in the Db, which happens when the Jg is 0.3, 0.5 and 1.0 cm/s the Db is 0.16, 0.13 and 0.11 cm in diameter, respectively.

As it can be seen in Figure 14, the bubble sizes are larger with respect to the tests where there is no pH control; however, from this difference, the silver(I) recoveries from the solution by ion flotation are relatively high, and larger bubbles will give a lower

Sb bubble surface area flux of about 50 (1/s), which is relatively lower than the tests previously described.

Regarding the apparent flotation kinetics (*k*) (1/min) maintains a similar behavior to the parameters of the gas dispersion in the continuous medium, where the increase in the gas holdup with the Jg (cm/s) also reduces the bubble size and the bubble specific surface area flux increases until reaching a maximum Sb of 50 (1/s) at Jg of 1.0 cm/s; these conditions allow us to obtain a *k* of 5.2 1/min.

Thus, the constant k is a function of the silver(I) recovery from the solution and in turn, the latter depends on the system chemistry modified by the addition of the appropriate frothers, collectors, and promoters, and the participation of the hydrodynamic conditions and dispersion properties.

3.2.4. Frother Dosage

The evaluation of the frother concentration on silver(I) recovery by ion flotation is presented in Figure 15 for both froth concentrations experimented 0.62×10^{-4} M and 1.25×10^{-4} M poly glycol ether PM400 with a of Jl 0.19 cm/s, 1.89×10^{-4} M [x], and 1.29×10^{-4} M [xl2945]. Similar extraction efficiencies are obtained except at Jg 1. 0 cm/s due to the turbulent bubble flux regime caused by the no homogeneous distribution of the bubbles in the flotation cell, generating higher circulation currents and increasing the residence time of the bubbles and thus decreasing the silver(I) recovery.

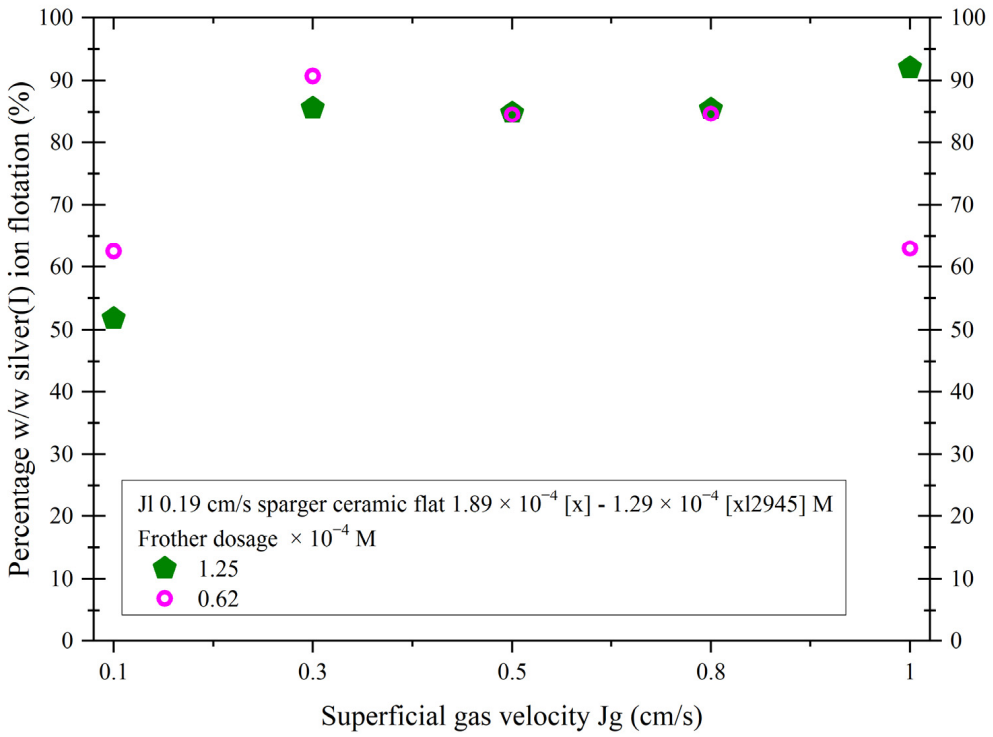

Figure 15. Percentage of *w*/*w* silver(I) recovery by ion flotation as function of superficial gas velocity, 1.89 collector–1.29 promoter $\times 10^{-4}$ M. Effect frother dosage, 0.62×10^{-4}, and 1.25×10^{-4} M, Jl 0.19 cm/s.

It can be established that silver(I) ion flotation systems with low frother concentration do not maintain the same separation efficiency at high Jg values (1.0 cm/s), as shown in Figure 15, when the flotation cell is operated with a Jg of 0. 3 cm/s the efficiency is high at around 90.7% *w*/*w* Ag recovery. This is derived from the physical properties generated from a lower concentration of frother (0.62×10^{-4} M) in the system in which the surface tension of the system is higher with respect to the 1.25×10^{-4} M frother concentration.

These differences in surface tension implies using more energy for bubble formation. In addition, the liquid film around the bubble may be less present and less resistance to coalescence and bubble recirculation. The dispersion properties of the maximum silver(I) recovery with 0.62 × 10^{-4} M of [e], 1.89 × 10^{-4} M [x], and 1.29 × 10^{-4} M [xl2945] are percentage of v/v Eg of 1.17, a Db of 0.25 cm, Sb of 6.96 cm/s, and an apparent flotation constant of 3. 8 (1/min), as shown in Figure 16, compared to the system where the separation efficiency is 92% w/w silver(I) recovery presents at Jg of 1.0 cm/s, Db of 0.18 cm, 50.5 (1/s) of Sb, and a k of 5.28 (1/min).

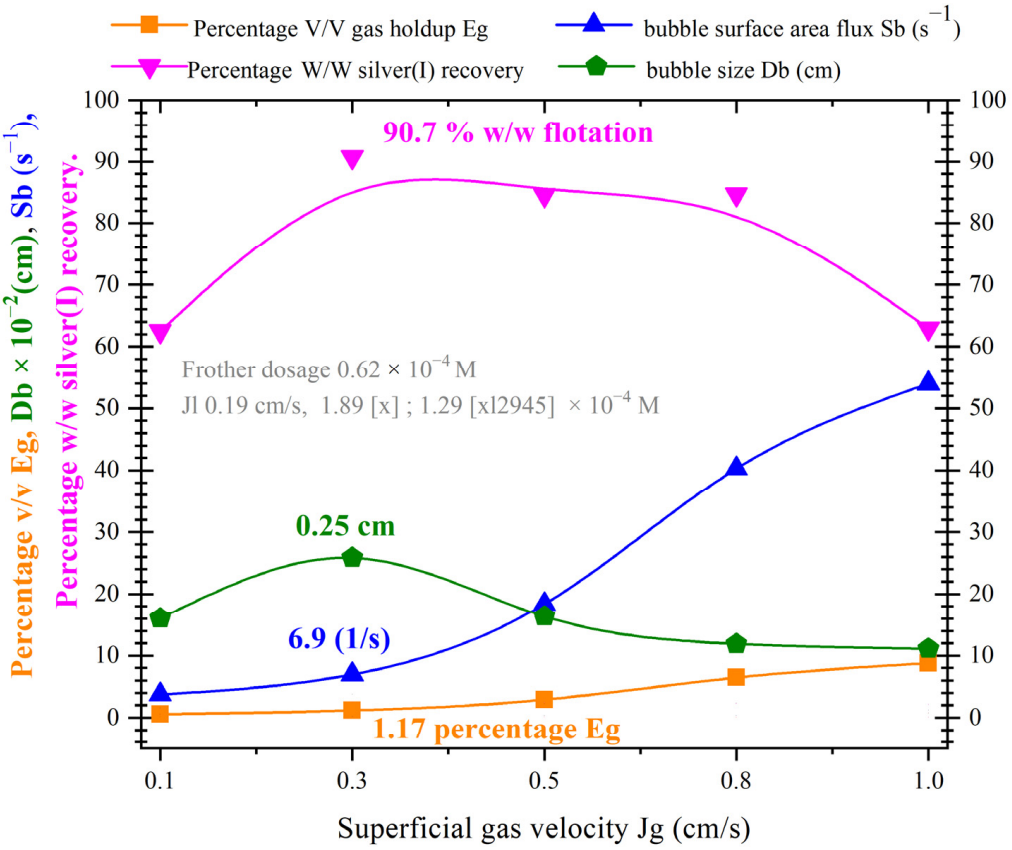

Figure 16. Eg, Db, Sb, and percentage of w/w of silver(I) ion flotation as function of superficial gas velocity, ceramic sparger, Jl 0.19 cm/s, system 1.89 × 10^{-4} M of [x]–1.29 × 10^{-4} M [xl2945], and [e] 0.62 × 10^{-4} M.

3.2.5. Evaluation of Geometry of the Dispersion System

Bubble spargers in sub-aerated flotation equipment can be either rigid, made of ceramic or porous stainless steel, or flexible, made of PVC pipe sections covered with synthetic fabric. In this section, the effect of using a separate rigid and flexible sparger on silver(I) extraction efficiency during ion flotation is analyzed.

Figure 17 shows the curves of the percentage of w/w silver(I) recovery as function of superficial gas velocity Jg (cm/s) in a system with a [e] of 1.25 × 10^{-4} M, 1.89 × 10^{-4} M of [x], and 1.29 × 10^{-4} M [xl2945] with a Jl of 0.19 cm/s for both rigid and flexible dispersion systems. It is clearly observable that higher recovery efficiencies are with the rigid sparger and are lower for the flexible spargers; this is due to the differences in the properties of the gas dispersion.

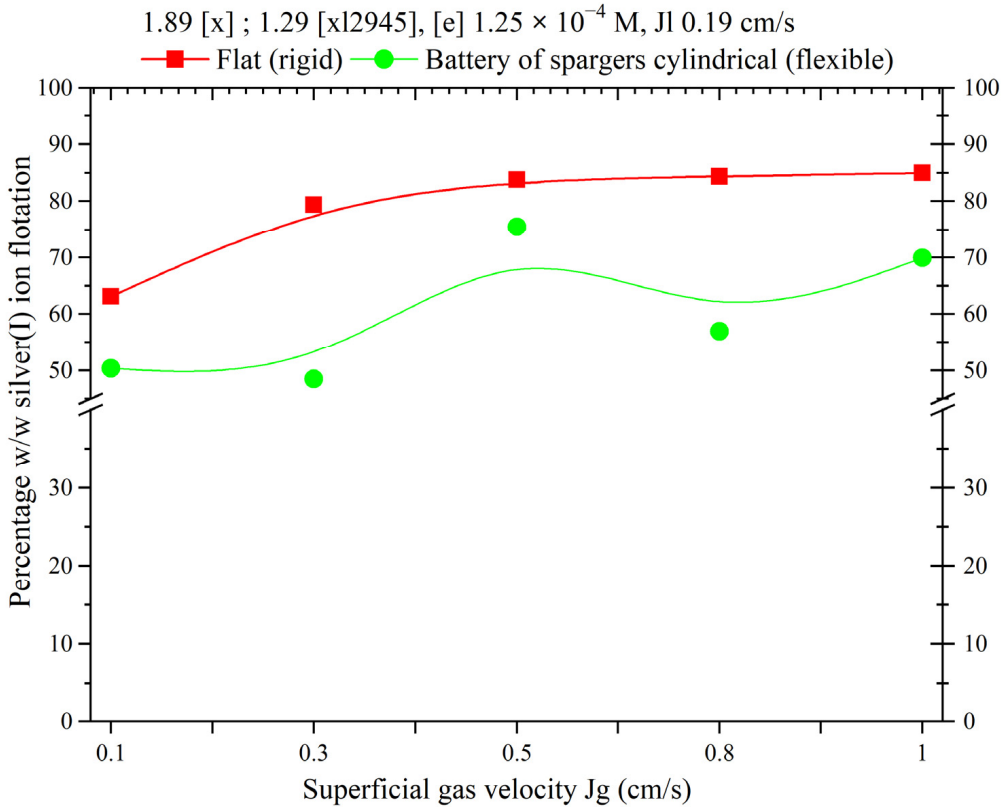

Figure 17. Percentage of w/w silver(I) recovery by ion flotation vs. superficial gas velocity, 1.89×10^{-4} M collector–1.29×10^{-4} M [xl2945], [e] 1.25×10^{-4} M, and Jl 0.19 cm/s.

The maximum silver(I) recovery obtained with the battery of three flexible bubble spargers is obtained at Jg of 0.5 cm/s with 75% w/w, and with increasing Jg, the percentage of w/w recovery decreases, while for the rigid sparger it is around 84% w/w silver(I) recovery and remains in a wide range of Jg.

The variation in silver(I) recoveries with the bubble generation system is mainly due to the value of the percentage of v/v of gas holdup, as shown in Figure 18, with the rigid sparger a higher Eg of about three times more than with the flexible sparger is obtained. For the flexible spargers battery, the linear behavior of Eg Vs Jg is lost when the Jg is 0. 8 cm/s or higher. This affects the mixing behavior inside the flotation cell going from a homogeneous bubble flux to a turbulent one, increasing the recirculation currents of the dispersed phase and the continuous phase directly influencing the silver(I) separation efficiency.

With the flexible sparger with a Jg of 1.5 cm/s, a maximum of 3% v/v Eg is obtained, while with the flat sparger is 10.6%. This variation is of consideration in the choice of the bubble dispersion system. Moreover, the behavior of Eg vs. Jg is maintained as a homogeneous flux of bubbles with moderate circulation currents and mixing of the continuous and dispersed phases.

Significant differences in Eg will also cause considerable variations in the bubble diameter, thus, larger bubble sizes cause, on one hand, a higher bubble ascent rate and therefore shorter residence time in the flotation cell, decreasing the probability of contact and collision between the hydrophobic species to be collected and the bubble. In addition, there will be less bubble specific surface area flux available to carry out the process.

Figure 19 shows the bubble diameter differences for both types of rigid and flexible spargers as a function of Jg (cm/s). For the flat sparger constructed of Shell molding sand (ceramic material), the Db's are on average 0.1 cm, while for the flexible sparger bubble, sizes are around 0. 36 cm; this larger size implies the decrease in the bubble specific surface area flux available to carry out the silver(I) recovery. However, these bubble sizes contribute

to decrease the time of the bubbles in the flotation cell, thus increasing the transfer rate of the hydrophobic silver(I) species from the liquid to the concentrate zone.

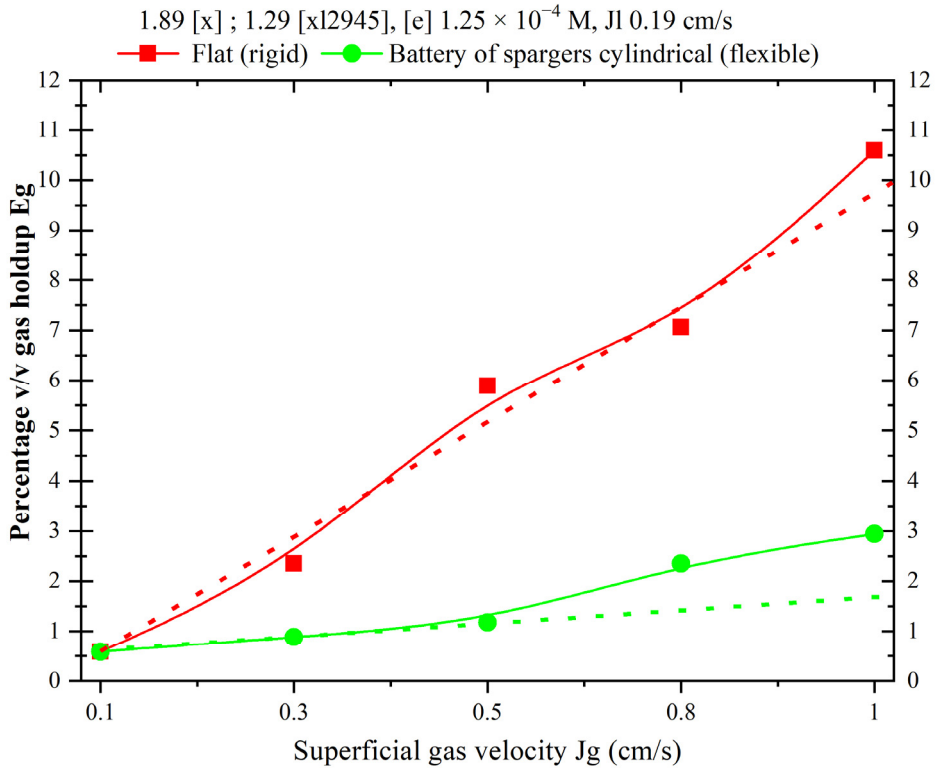

Figure 18. The effect of dispersion gas system percentage of v/v gas holdup as function of superficial gas velocity Jg (cm/s), 1.89 × 10^{-4} M [x], 1.29 × 10^{-4} M [xl2945], and [e] 1.25 × 10^{-4} M.

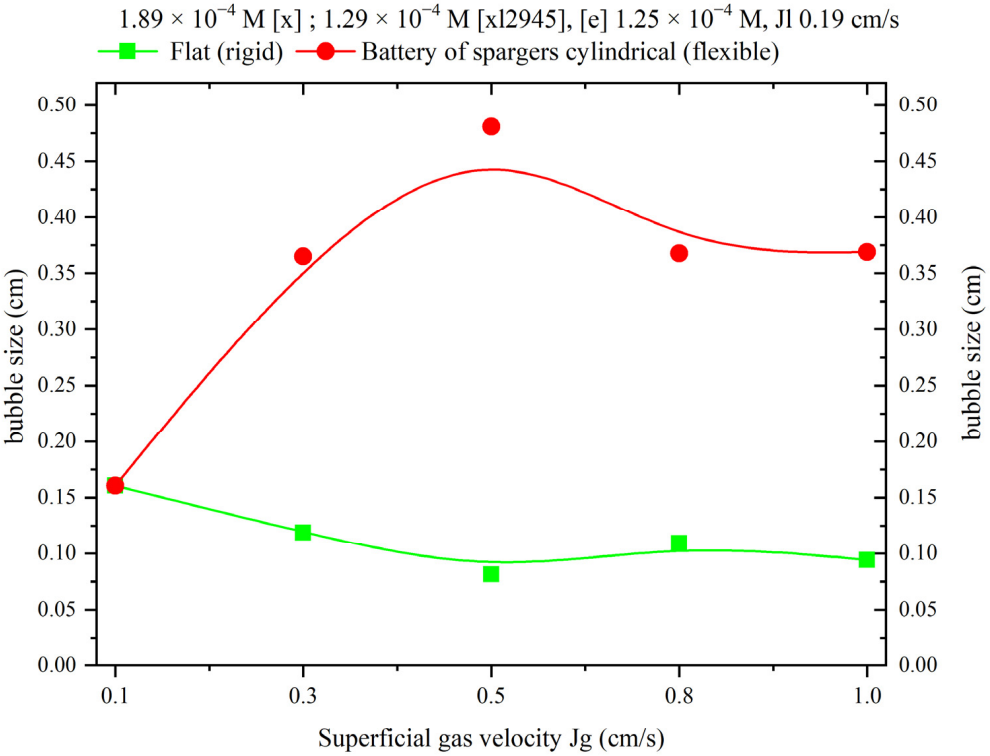

Figure 19. The effect of dispersion gas system bubble size (cm) vs. superficial gas velocity, Jg (cm/s), 1.89 × 10^{-4} M [x], 1.29 × 10^{-4} M [xl2945], and [e] 1.25 × 10^{-4} M.

Regarding the apparent flotation kinetic constant approximated to a first order equation, Figure 20 shows the behavior as a function of different concentrations of collector, promoter, pH, and frother agent. Figure 20 shows that the use of only xanthate allows the flotation cell to operate at a maximum of Jg 0.5 cm/s; subsequently, the flotation constant decreases, while the use of promoter-collector combinations, and keeping the pH constant. The ion flotation allows for the operate of the flotation cell with values of Jg equal to 1.0 cm/s. The detriment of the ionic flotation occurs when exclusively concentration combinations of dithiophosphate and dithiophosphinate promoters are used.

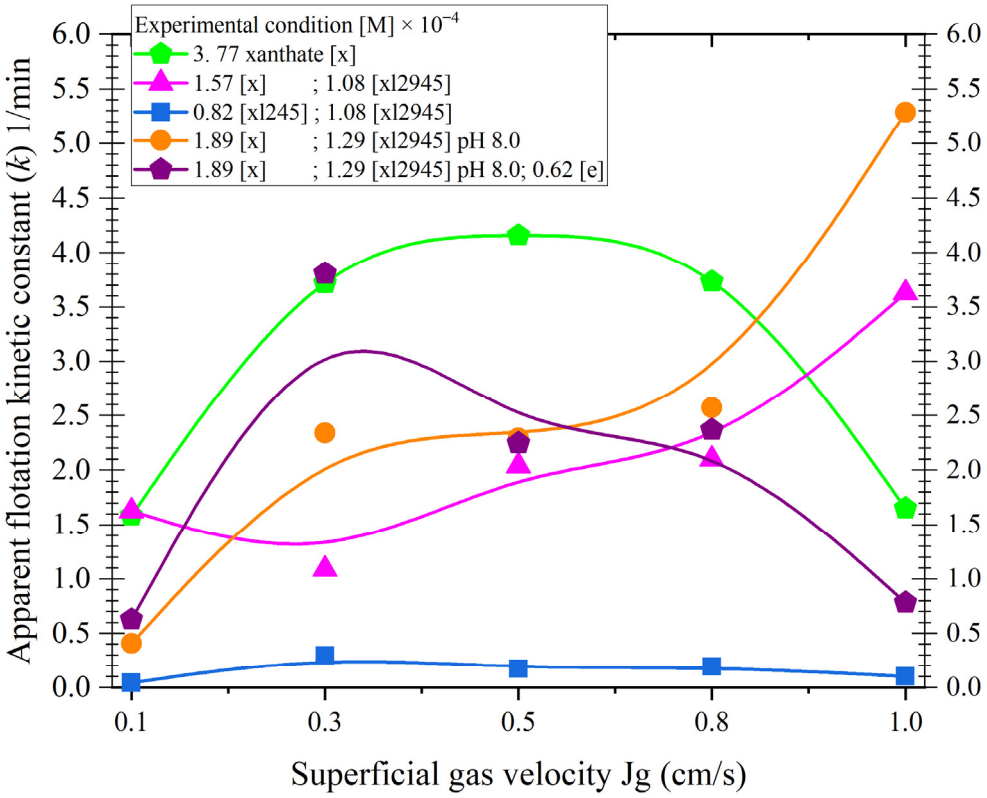

Figure 20. Apparent flotation kinetic constant (K) 1/min as function of superficial gas velocity. For different experimental conditions.

4. Conclusions

Silver(I) extraction from diluted aqueous solutions was carried out with ion flotation techniques in sub-aerated cells with rigid and flexible porous spargers. Silver(I) recovery was analyzed as a function of dispersion properties, gas surface velocity Jg (cm/s), percentage of v/v gas holdup Eg, bubble diameter Db (cm), bubble specific surface area flux Sb (1/s), and the apparent flotation kinetics k (1/min).

The analysis of the hydrodynamic behavior of the flotation cell showed that the cell can be operated in a homogeneous and stable bubble flux regime in a Jg range of 0.1 to 0.5 cm/s. In addition, Eg and Db are not uniformly distributed in the equipment generating circulation and mixing currents that influence the extraction of silver(I) from the solution.

A xanthate concentration of 3.77×10^{-4} M allows to extract 90.7% w/w silver(I), with optimum dispersion properties of: 4.1% v/v Eg, Db 0.11 (cm), Sb 26.1 (1/s), and a flotation constant k (1/min) of 4.1. Combinations with xanthate [x]—promoter either 0.82×10^{-4} M [xl245] or 1.08×10^{-4} M [xl2945]—allows for the extension of the operating range of Jg in the flotation cell, obtained at Jg of 1.0 cm/s with a percentage of w/w silver(I) extraction of 86.9%.

If the pH of the solution is kept constant at 8.0, and the collector is 1.89×10^{-4} M [x] and the promoter is 1.29×10^{-4} M [xl2945], the silver(I) extraction can reach 92% with a Jg

of 1.0 cm/s. These physical and chemical conditions give a percentage of v/v Eg of 8.2%, Db 0.11 (cm), Sb 50.5 (1/s), and a flotation constant k (1/min) of 5.2. The decrease in the frother concentration, [e] 0.62×10^{-4} M, during ion flotation affects the percentage of w/w silver(I) recovery, achieving 62.9% and decreasing the operating Jg of the cell to 0.8 cm/s. For silver(I) recovery by ion flotation, a rigid porous ceramic sparger is recommended with flexible spargers to generate bubble sizes of about 0.36 cm.

Supplementary Materials: The following supporting information can be downloaded at: https://www.mdpi.com/article/10.3390/min13040572/s1, Table S1: Calibration of the peristaltic feed. Table S2: Calibration of the peristaltic discharge pump (tails). Table S3: Calculation of gas surface velocity Jg (cm/s). Bubble Diameter Estimation Using the Drift Flux Model. docx [30–33].

Author Contributions: Formal analysis, M.U.F.G.; investigation, L.P.Á.P., M.R.P., I.A.R.D., F.R.B.H. and M.P.L.; methodology, F.P.C. and J.C.J.T.; supervision, R.E.G. All authors have read and agreed to the published version of the manuscript.

Funding: This research received no external funding.

Conflicts of Interest: The authors declare no conflict of interest.

References

1. Arslan, F.; Bulut, G. Ion flotation and its applications on concentration, recovery, and removal of metal ions from solutions. *Physicochem. Probl. Miner. Process.* **2022**, *58*, 152061. [CrossRef]
2. Reyes, M.; Patiño, F.; Escudero, R.; Pérez, M.; Flores, M.U.; Reyes, I.A. Kinetics and hydrodynamics of silver ion flotation. *J. Mex. Chem. Soc.* **2012**, *56*, 408–416.
3. Zouboulis, A.I. Silver recovery from aqueous streams using ion flotation. *Miner. Eng.* **1995**, *8*, 1477–1488. [CrossRef]
4. Ahlatci, F.I.R.A.T.; Yazici, E.Y.; Yilmaz, E.L.I.F.; Celep, O.K.T.A.Y.; Deveci, H.A.C.I. A novel method for the recovery of silver from thiosulphate leach solutions using trimercapto-s-triazine (TMT). *Miner. Eng.* **2022**, *177*, 107373. [CrossRef]
5. Charewicz, W.A.; Holowiecka, B.A.; Walkowiak, W. Selective flotation of zinc (II) and silver (I) ions from dilute aqueous solutions. *Sep. Sci. Technol.* **1999**, *34*, 2447–2460. [CrossRef]
6. Reyes, M.; Patiño, F.; Tavera, F.J.; Escudero, R.; Rivera, I.; Pérez, M. Kinetics and recovery of xanthate-copper compounds by ion flotation techniques. *J. Mex. Chem. Soc.* **2009**, *53*, 15–22. [CrossRef]
7. Ahmed, S.H.; El Gammal, E.M.; Amin, M.I.; Yousef, W.M. Studying the Effect of Potassium Amyl Xanthate Surfactant on Fe, Cu and U Ions for the Pretreatment of Abu Zeneima Sulphate Leach Liquor. *Period. Polytech. Chem. Eng.* **2021**, *65*, 408–415. [CrossRef]
8. Hoseinian, F.S.; Rezai, B.; Kowsari, E.; Safari, M. Kinetic study of Ni (II) removal using ion flotation: Effect of chemical interactions. *Miner. Eng.* **2018**, *119*, 212–221. [CrossRef]
9. Khatir, M.Z.; Abdollahy, M.; Khalesi, M.R.; Rezai, B. The selective separation of neodymium from aluminum using ion flotation. *Miner. Eng.* **2022**, *180*, 107480. [CrossRef]
10. Yenial, Ü.; Bulut, G. Examination of flotation behavior of metal ions for process water remediation. *J. Mol. Liq.* **2017**, *241*, 130–135. [CrossRef]
11. Nafi, A.W.; Taseidifar, M. Removal of hazardous ions from aqueous solutions: Current methods, with a focus on green ion flotation. *J. Environ. Manag.* **2022**, *319*, 115666. [CrossRef] [PubMed]
12. Chang, L.; Cao, Y.; Fan, G.; Li, C.; Peng, W. A review of the applications of ion floatation: Wastewater treatment, mineral beneficiation and hydrometallurgy. *RSC Adv.* **2019**, *9*, 20226–20239. [CrossRef] [PubMed]
13. Hoseinian, F.S.; Rezai, B.; Safari, M.; Deglon, D.; Kowsari, E. Effect of hydrodynamic parameters on nickel removal rate from wastewater by ion flotation. *J. Environ. Manag.* **2019**, *244*, 408–414. [CrossRef] [PubMed]
14. Sebba, F. Concentration by ion flotation. *Nature* **1959**, *184*, 1062–1063. [CrossRef]
15. Peng, W.; Chang, L.; Li, P.; Han, G.; Huang, Y.; Cao, Y. An overview on the surfactants used in ion flotation. *J. Mol. Liq.* **2019**, *286*, 110955. [CrossRef]
16. Deliyanni, E.A.; Kyzas, G.Z.; Matis, K.A. Various flotation techniques for metal ions removal. *J. Mol. Liq.* **2017**, *225*, 260–264. [CrossRef]
17. Demissie, H.; Lu, S.; Jiao, R.; Liu, L.; Xiang, Y.; Ritigala, T.; Ajibade, F.O.; Mihiranga, H.K.M.; An, G.; Wang, D. Advances in micro interfacial phenomena of adsorptive micellar flocculation: Principles and application for water treatment. *Water Res.* **2021**, *202*, 117414. [CrossRef]
18. Bulatovic, S.M. *Handbook of Flotation Reagents: Chemistry, Theory and Practice: Volume 1: Flotation of Sulfide Ores*; Elsevier: Amsterdam, The Netherlands, 2007.
19. Grieves, R.B.; Bhattacharyya, D.; Ghosal, J.K. Surfactant-colligend particle size effects on ion flotation: Influences of mixing time, temperature, and surfactant chain length. *Colloid Polym. Sci.* **1976**, *254*, 507–515. [CrossRef]
20. Lobacheva, O.; Dzhevaga, N.; Danilov, A. The method of removal yttrium (III) and ytterbium (III) from dilute aqueous solutions. *J. Ecol. Eng.* **2016**, *17*, 62284. [CrossRef]

21. Taseidifar, M.; Makavipour, F.; Pashley, R.M.; Rahman, A.M. Removal of heavy metal ions from water using ion flotation. *Environ. Technol. Innov.* **2017**, *8*, 182–190. [CrossRef]
22. Polat, H.; Erdogan, D. Heavy metal removal from waste waters by ion flotation. *J. Hazard. Mater.* **2007**, *148*, 267–273. [CrossRef] [PubMed]
23. Galvin, K.P.; Engel, M.D.; Nicol, S.K. The potential for reagent recycle in the ion flotation of gold cyanide—A pilot scale field trial. *Int. J. Miner. Process.* **1994**, *42*, 75–98. [CrossRef]
24. Walkowiak, W.; Ulewicz, M. Kinetics studies of ion flotation. *Fizykochem. Probl. Miner.* **1999**, *33*, 201–214.
25. Walkowiak, W. Mechanism of selective ion flotation. 1. Selective flotation of transition metal cations. *Sep. Sci. Technol.* **1991**, *26*, 559–568. [CrossRef]
26. Girek, T.; Kozlowski, C.A.; Koziol, J.J.; Walkowiak, W.; Korus, I. Polymerisation of β-cyclodextrin with succinic anhydride. Synthesis, characterisation, and ion flotation of transition metals. *Carbohydr. Polym.* **2005**, *59*, 211–215. [CrossRef]
27. Finch, J.A.; Dobby, G.S. *Column Flotation*; Pergamon Press: Oxford, UK, 1990.
28. Tavera, F.J.; Escudero, R.; Uribe, A.; Finch, J.A. Ni-DETA flotation in aqueous media: Application of flotation columns. *Afinidad* **2000**, *57*, 415–423.
29. Gorain, B.K.; Franzidis, J.P.; Manlapig, E.V. *Flotation Cell Design: Application of Fundamental Principles*; Julius Kruttschnitt Mineral Research Centre: Indooroopilly, QLD, Australia, 2000; pp. 1502–1512.
30. Tavera, F.J.; Gómez, C.O.; Finch, J.A. Conductivity flow cells for measurements on dispersions. *Can. Metall. Q.* **1998**, *37*, 19–25. [CrossRef]
31. Tavera, F.J.; Escudero, R. Gas hold-up and solids hold-up in flotation columns: On-line measurement based on electrical conductivity. *Miner. Process. Extr. Metall.* **2002**, *111*, 94–99. [CrossRef]
32. Tavera, F.J.; Gomez, C.O.; Finch, J.A. Estimation of gas holdup in froths by electrical conductivity: Application of the standard addition method. *Miner. Eng.* **1998**, *11*, 941–947. [CrossRef]
33. Tavera, F.J.; Escudero, R.; Finch, J.A. Gas holdup in flotation columns: Laboratory measurements. *Int. J. Miner. Process.* **2001**, *61*, 23–40. [CrossRef]
34. Celep, O.; Altinkaya, P.; Yazici, E.Y.; Deveci, H. Thiosulphate leaching of silver from an arsenical refractory ore. *Miner. Eng.* **2018**, *122*, 285–295. [CrossRef]
35. Dobby, G.S.; Yianatos, J.B.; Finch, J.A. Estimation of bubble diameter in flotation columns from drift flux analysis. *Can. Metall. Q.* **1988**, *27*, 85–90. [CrossRef]
36. Yianatos, J.B.; Finch, J.A.; Laplante, A.R. Holdup profile and bubble size distribution of flotation column froths. *Can. Metall. Q.* **1986**, *25*, 23–29. [CrossRef]
37. Gomez, C.O.; Maldonado, M. Modelling Bubble Flow Hydrodynamics: Drift-Flux and Molerus Models. *Minerals* **2022**, *12*, 1502. [CrossRef]
38. Lelinski, D.; Allen, J.; Redden, L.; Weber, A. Analysis of the residence time distribution in large flotation machines. *Miner. Eng.* **2002**, *15*, 499–505. [CrossRef]
39. Xu, M.; Finch, J.A. Effect of sparger surface area on bubble diameter in flotation columns. *Can. Metall. Q.* **1989**, *28*, 1–6. [CrossRef]